



IN THE UNITED STATES PATENT AND TRADEMARK OFFICE

In re Patent Application of

ARDAVAN et al.

Atty. Ref.: 117-342; Confirmation No.

Appl. No. 09/786,507

TC/A.U. 2881

Filed: March 6, 2001

Examiner: B. Souw

For: APPARATUS FOR GENERATING FOCUSED ELECTROMAGNETIC
RADIATION

* * * * *

Commissioner for Patents
P.O. Box 1450
Alexandria, VA 22313-1450

Sir:

DECLARATION UNDER 37 CFR §1.132

I, Dr. Dwight Rickel, hereby declare that:

1. I have been an applied physicist for the past 35 years and have considerable knowledge and experience in electromagnetics and propagation phenomenon. Specifically, I spent two years measuring electromagnetic emissions from relativistic electron beams propagating in air where ground reflections and antenna calibrations were of considerable importance. I was also involved in wideband antenna development and ionospheric propagation.

2. Since 1980, I have worked at Los Alamos National Laboratory¹ in areas related to nuclear physics. In 1991, I was the project leader that built the National High Magnetic Field Laboratory at Los Alamos. Since 1991, I have worked as a staff scientist in the National High Magnetic Field Laboratory. Prior to working at Los Alamos National Laboratory, I worked at a company called EE&G in ionospheric physics and RF propagation and at Northrup Services working on long path monitoring for lasers. I received my Masters of Science (nuclear physics) in 1971 and a PhD. (nuclear physics) in 1973 from the University of Arizona. I was a post doctoral fellow at Duke University for approximately two years in nuclear physics.

3. Based on my considerable education and experience in electromagnetics and propagation phenomenon, I believe myself to be an expert in the technological area of U.S. Patent Application Serial No. 09/786,507, entitled: "Apparatus For Generating Focused Electromagnetic Radiation" (the '507 application).

4. I have reviewed the '507 application as originally filed, (attached as Exhibit A), the Examiner's Official Action dated December 15, 2003, (attached as Exhibit B), a document entitled "Description of an Experiment: Response to the First Office Action by the U.S. Patent Office on the Application No. 09/786,507," (attached as Exhibit C), and a document entitled "Description of Some Experimental Results: Response to the First Office Action by the U.S. Patent Office on the Application No. 09/786,507," (attached as Exhibit D).

¹ This is my personal declaration and does not represent any official involvement of the Los Alamos

5. The '507 application claim 21 recites an apparatus for generating electromagnetic radiation that includes polarizable or magnetization medium and a means for generating in a controlled manner a polarization or magnetization current or charge distribution. The current distribution has an accelerated motion with a superluminal speed that generates non-spherically decaying electromagnetic radiation whose intensity falls off at a rate at or about $1/R$ in the far field. R is the distance from the current distribution. This fall off rate or attenuation is considerably less than the rate at which the intensity electromagnetic radiation normally falls off, i.e., $1/R^2$.

6. The invention described in the '507 application has an extremely wide range of applications. Some examples include high bandwidth telecommunications, secure communications, hand-held communication devices, compact sources of intense broad band radiation, medical diagnoses and treatments, and biomedical research. Of course, there are many other applications.

7. The Examiner contends that the principles described and claimed in the '507 application violate the special theory of relativity. The claimed invention does not violate relativity principles because the electromagnetic radiation itself is not described or claimed to be traveling at greater than the speed of light. Rather, it is the current distribution, which is the source of the EM radiation, that can achieve superluminal speed. An example of a phenomenon that travels at a speed greater than light is a pair of

scissors whose tips are moving just below the speed of light. In this situation, the intersection of the blades moves at a speed faster than the speed of light.

8. Regarding the non-spherical decay recited in claim 21, it can be demonstrated using Huygens wavelets that there are locations where multiple waves from of the source of radiation (the current or charge distribution) can simultaneously arrive at a point in space, labeled a "cusp" in the '507 application, which create a higher than usual intensity due to constructive interference. Moving away from the distribution, more wavelets converge on the cusp giving rise to non-spherical decay in the far field better than $1/R^2$. Because there is constructive interference at these cusp points and destructive interference elsewhere, the amount of energy passing through any given spherical surface surrounding the current or charge distribution is constant. Thus, conservation of energy is not violated.

9. The Examiner improperly characterizes the invention as nothing more than laser beaming or a phased array antenna. The intensity of laser radiation diminishes with the distance R from its source like $1/R^2$ in the far field, i.e., where R is greater than the Fresnel distance. Thus, laser radiation decays spherically rather than non-spherically. Moreover, the claimed apparatus is not just another phased array because it generates an intense energy cusp as described in the specification and illustrated in Figures 3, 4, and 9.

10. After reviewing the experiment described in Exhibit C, I have determined that the instrumentation was properly configured and the testing conducted in accordance with standard scientific procedures. I have reviewed the experimental test results as set

forth in Exhibit D and have determined that the data interpretation was correct.

Specifically, appropriate consideration was given to common mode rejection from transmission lines and to ground reflections.

11. Figure 1 in Exhibit D illustrates the intensity versus distance on a log scale for radiation generated by a subluminal (slower than the speed of light) current distribution. Figure 2 Exhibit D illustrates the radiation intensity versus distance generated by a charge or current distribution having superluminal speed. Figure 3 Exhibit D illustrates the ratio of the radiation intensity at superluminal speed over the radiation intensity at subluminal speed. The radiation intensity in Figure 1 decays at a rate of approximately $1/R^2$ once account is taken of interference from the ground, while the slope of a line corresponding to that ratio confirms that the intensity in Figure 2 decays at a rate of approximately $1/R$, where R is the distance from the charge or current distribution.

12. All statements made herein of my own knowledge are true, and those made on information and belief are believed to be true. These statements were made with the knowledge that willful false statements are punishable by fine or imprisonment, or both, under '1001 of Title 18 of the United States Code, and that such willful false statements may jeopardize the validity of the application or any patent issuing thereon.

Date: May 13, 2004

By: 
Dr. Dwight Rickel



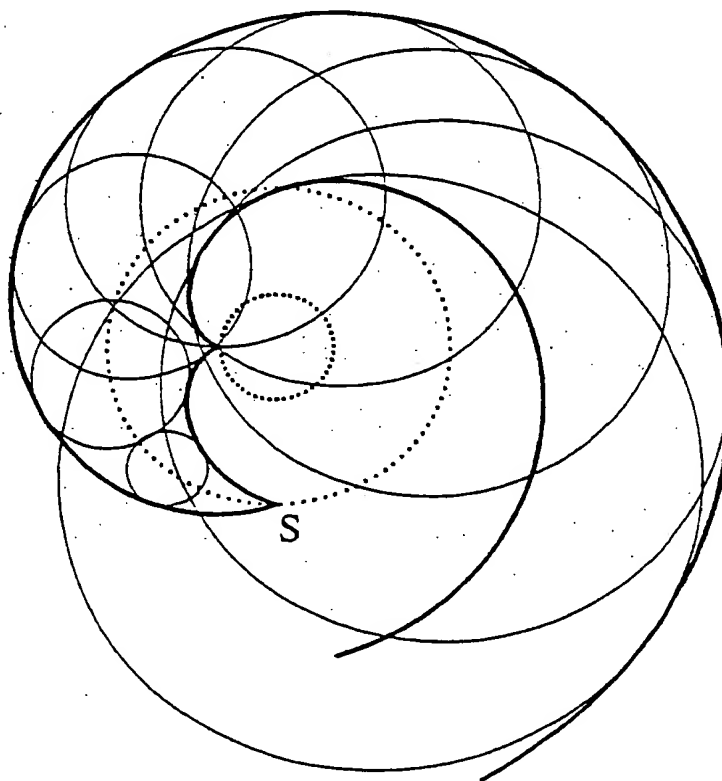
INTERNATIONAL APPLICATION PUBLISHED UNDER THE PATENT COOPERATION TREATY (PCT)

(51) International Patent Classification ⁷ : G21K 1/16, 1/00		A1		(11) International Publication Number: WO 00/14750
				(43) International Publication Date: 16 March 2000 (16.03.00)
(21) International Application Number: PCT/GB99/02943		(81) Designated States: AE, AL, AM, AT, AU, AZ, BA, BB, BG, BR, BY, CA, CH, CN, CR, CU, CZ, DE, DK, DM, EE, ES, FI, GB, GD, GE, GH, GM, HR, HU, ID, IL, IN, IS, JP, KE, KG, KP, KR, KZ, LC, LK, LR, LS, LT, LU, LV, MD, MG, MK, MN, MW, MX, NO, NZ, PL, PT, RO, RU, SD, SE, SG, SI, SK, SL, TJ, TM, TR, TT, UA, UG, US, UZ, VN, YU, ZA, ZW, ARIPO patent (GH, GM, KE, LS, MW, SD, SL, SZ, UG, ZW), Eurasian patent (AM, AZ, BY, KG, KZ, MD, RU, TJ, TM), European patent (AT, BE, CH, CY, DE, DK, ES, FI, FR, GB, GR, IE, IT, LU, MC, NL, PT, SE), OAPI patent (BF, BJ, CF, CG, CI, CM, GA, GN, GW, ML, MR, NE, SN, TD, TG).		
(22) International Filing Date: 6 September 1999 (06.09.99)				
(30) Priority Data: 9819504.3 7 September 1998 (07.09.98) GB				
(71)(72) Applicants and Inventors: ARDAVAN, Arzhang [GB/GB]; Wolfson College, Linton Road, Oxford OX2 6UD (GB). ARDAVAN, Houshang [GB/GB]; New Hall, Huntingdon Road, Cambridge CB3 0DF (GB).				
(74) Agent: GILL JENNINGS & EVERY; Broadgate House, 7 Eldon Street, London EC2M 7LH (GB).		Published <i>With international search report. Before the expiration of the time limit for amending the claims and to be republished in the event of the receipt of amendments.</i>		

(54) Title: APPARATUS FOR GENERATING FOCUSED ELECTROMAGNETIC RADIATION

(57) Abstract

An apparatus for generating electromagnetic radiation comprises a polarizable or magnetizable medium. There is means of generating, in a controlled manner, a polarization or magnetisation current whose distribution pattern has an accelerated motion with a superluminal speed, so that the apparatus generated both a non-spherically decaying component and an intense spherically decaying component of electromagnetic radiation.



FOR THE PURPOSES OF INFORMATION ONLY

Codes used to identify States party to the PCT on the front pages of pamphlets publishing international applications under the PCT.

AL	Albania	ES	Spain	LS	Lesotho	SI	Slovenia
AM	Armenia	FI	Finland	LT	Lithuania	SK	Slovakia
AT	Austria	FR	France	LU	Luxembourg	SN	Senegal
AU	Australia	GA	Gabon	LV	Latvia	SZ	Swaziland
AZ	Azerbaijan	GB	United Kingdom	MC	Monaco	TD	Chad
BA	Bosnia and Herzegovina	GE	Georgia	MD	Republic of Moldova	TG	Togo
BB	Barbados	GH	Ghana	MG	Madagascar	TJ	Tajikistan
BE	Belgium	GN	Guinea	MK	The former Yugoslav Republic of Macedonia	TM	Turkmenistan
BF	Burkina Faso	GR	Greece			TR	Turkey
BG	Bulgaria	HU	Hungary	ML	Mali	TT	Trinidad and Tobago
BJ	Benin	IE	Ireland	MN	Mongolia	UA	Ukraine
BR	Brazil	IL	Israel	MR	Mauritania	UG	Uganda
BY	Belarus	IS	Iceland	MW	Malawi	US	United States of America
CA	Canada	IT	Italy	MX	Mexico	UZ	Uzbekistan
CF	Central African Republic	JP	Japan	NE	Niger	VN	Viet Nam
CG	Congo	KE	Kenya	NL	Netherlands	YU	Yugoslavia
CH	Switzerland	KG	Kyrgyzstan	NO	Norway	ZW	Zimbabwe
CI	Côte d'Ivoire	KP	Democratic People's Republic of Korea	NZ	New Zealand		
CM	Cameroon			PL	Poland		
CN	China	KR	Republic of Korea	PT	Portugal		
CU	Cuba	KZ	Kazakhstan	RO	Romania		
CZ	Czech Republic	LC	Saint Lucia	RU	Russian Federation		
DE	Germany	LI	Liechtenstein	SD	Sudan		
DK	Denmark	LK	Sri Lanka	SE	Sweden		
EE	Estonia	LR	Liberia	SG	Singapore		

APPARATUS FOR GENERATING FOCUSED
ELECTROMAGNETIC RADIATION

The present invention relates to the generation of electromagnetic radiation and, more particularly, to an apparatus and method of generating focused pulses of electromagnetic radiation over a wide range of frequencies. More particularly it relates to an apparatus and method for generating pulses of non-spherically decaying electromagnetic radiation.

The present apparatus and method are based on the emission of electromagnetic radiation by rapidly varying polarisation or magnetisation current distributions rather than by conduction or convection electric currents. Such currents can have distribution patterns that move with arbitrary speeds (including speeds exceeding the speed of light *in vacuo*), and so can radiate more intensely over a much wider range of frequencies than their conventional counterparts. The spectrum of the radiation they generate could extend to frequencies that are by many orders of magnitude higher than the characteristic frequency of the fluctuations of the source itself.

Furthermore, intensities of normal emissions decay at a rate of R^{-2} , where R is the distance from the source. It has been noted, however, that the intensities of certain pulses of electromagnetic radiation can decay spatially at a lower rate than that predicted by this inverse square law (see Myers *et al.*, Phys. World, Nov. 1990, p. 39). The new solution of Maxwell's equations set out below, for example, predicts that the electromagnetic radiation emitted from superluminally, circularly moving charged patterns decays at a rate of R^{-1} . Another example is the electromagnetic radiation emitted from superluminally, rectilinearly moving charged patterns which decays at a rate of $R^{-\frac{1}{2}}$.

This emission process can be exploited, moreover, to generate waves which do not form themselves into a focused pulse until they arrive at their intended destination and which subsequently remain in focus only for an adjustable interval of time.

It will be widely appreciated that being able to employ such emissions for signal transmission, amongst other applications, would have significant commercial value, given that it would enable the employment of lower power transmitters and/or larger transmission ranges, the use of signals that cannot be intercepted by third parties, and the exploitation of higher bandwidth. The near-field component of the radiation in question has many features in common with, and so can be used as an alternative to, synchrotron radiation. The present invention provides a method and apparatus for generating such emissions.

According to the present invention there is provided an apparatus for

generating electromagnetic radiation comprising:

a polarizable or magnetizable medium; and

means of generating, in a controlled manner, a polarisation or magnetisation current with a rapidly moving, accelerating distribution pattern such that the moving source in question generates electromagnetic radiation.

The speed of the moving distribution pattern may be superluminal so that the apparatus generates both a non-spherically decaying component and an intense spherically decaying component of electromagnetic radiation.

The apparatus may comprise a dielectric substrate, a plurality of electrodes positioned adjacent to the substrate, and the means for applying a voltage to the electrodes sequentially at a rate sufficient to induce a polarised region in the substrate which moves along the substrate with a speed exceeding the speed of light. The dielectric substrate may have either a rectilinear or a circular shape.

The wavelength of the generated electromagnetic radiation may be in any range from the radio to a minimum determined only by the lower limit to the acceleration of the source (potentially optical, ultraviolet or even x-ray).

Examples of the present invention will now be described with reference to the accompanying drawings, in which:

Figure 1 is a diagram showing the wave fronts of the electromagnetic emission from a particular volume element (source point) *S* within the circularly moving polarised region of the polarizable medium of the present invention;

Figure 2 is a graph showing the value of a function representing the emission time versus the retarded position for differing source points *a*, *b*, *c* within the polarizable medium in question;

Figure 3 is a perspective view of the envelope of the wave fronts shown in Fig. 1;

Figure 4 is a view of the cusp curve of the envelope shown in Fig. 3;

Figure 5 is the locus of the possible source points which approach the observation point *P* along the radiation direction with the wave speed at the retarded time, a locus that is henceforth referred to as the bifurcation surface of the observer at *P*;

Figure 6 is a view of the cross sections of the bifurcation surface and the source distribution with a cylinder whose axis coincides with the rotation axis of the source;

Figures 7(a) and 7(b) are views of two examples of the apparatus of the present invention showing the dielectric substrate, the electrodes and a superluminally moving polarised region of the dielectric substrate;

Figure 8 is a diagram showing the wave fronts, and the envelope of the wave fronts, of the electromagnetic emission from a particular volume element

(source point) S within the rectilinearly moving, accelerating superluminal source of the present invention; and

Figure 9 shows the evolution in observation time of the relative positions and the envelope of a set of wave fronts emitted during a limited interval of retarded time; the snapshots (a)-(f) include times at which the envelope has not yet developed a cusp [(a) and (b)], has a cusp [(c)-(e)], and has already lost its cusp (f).

Prior to description of the invention, it is appropriate to discuss the principles underlying it.

Bolotovskii and Ginzburg (Soviet Phys. Usp. 15, 184, 1972) and Bolotovskii and Bykov (Soviet Phys. Usp. 33, 477, 1990) have shown that the coordinated motion of aggregates of charged particles can give rise to extended electric charges and currents whose distribution patterns propagate with a phase speed exceeding the speed of light *in vacuo* and that, once created, such propagating charged patterns act as sources of the electromagnetic fields in precisely the same way as any other moving sources of these fields. That these sources travel faster than light is not, of course, in any way incompatible with the requirements of special relativity. The superluminally moving pattern is created by the coordinated motion of aggregates of subluminally moving particles.

We have solved Maxwell's equations for the electromagnetic field that is generated by an extended source of this type in the case where the charged pattern rotates about a fixed axis with a constant angular frequency.

There are solutions of the homogeneous wave equation referred to, *inter alia*, as non-diffracting radiation beams, focus wave modes or electromagnetic missiles, which describe signals that propagate through space with unexpectedly slow rates of decay or spreading. The potential practical significance of such signals is clearly enormous. The search for *physically realizable* sources of them, however, has so far remained unsuccessful. Our calculation pinpoints a concrete example of the sources that are currently looked for in this field by establishing a physically tenable *inhomogeneous* solution of Maxwell's equations with the same characteristics.

Investigation of the present emission process was originally motivated by the observational data on pulsars. The radiation received from these celestial sources of radio waves consists of highly coherent pulses (with as high a brightness temperature as 10^{30} °K) which recur periodically (with stable periods of the order of 1 sec). The intense magnetic field ($\sim 10^{12}$ G) of the central neutron star in a pulsar affects a coupling between the rotation of this star and that of the distribution pattern of the plasma surrounding it, so that the magnetospheric charges and currents in these objects are of the same type as those described above. The effect responsible for the extreme

degree of coherence of the observed emission from pulsars, therefore, may well be the violation of the inverse square law that is here predicted by our calculation.

The present analysis is relevant also to the mathematically similar problem of the generation of acoustic radiation by supersonic propellers and helicopter rotors, although this is not discussed in detail here.

We begin by considering the waves that are emitted by an element of the superluminally rotating source from the standpoint of geometrical optics. Next, we calculate the amplitudes of these waves, i.e. the Green's function for the problem, from the retarded potential. We then specify the bifurcation surface of the observer and proceed to calculate the electromagnetic radiation arising from a superluminally moving *extended* source. The singularities of the integrands of the radiation integrals that occur on the bifurcation surface are here handled by means of the theory of generalised functions: the electric and magnetic fields are given by the Hadamard's finite parts of the divergent integrals that result from differentiating the retarded potential under the integral sign. The theory is then concluded with a descriptive account of the analysed emission process in more physical terms, the description of examples of the apparatus, and an outline of the applications of the invention.

1. ENVELOPE OF THE WAVE FRONTS AND ITS CUSP

Consider a point source (an element of the propagating distribution pattern of a volume source) which moves on a circle of radius r with the constant angular velocity $\omega \hat{e}_z$, i.e. whose path $\mathbf{x}(t)$ is given, in terms of the cylindrical polar coordinates (r, φ, z) , by

$$r = \text{const.}, \quad z = \text{const.}, \quad \varphi = \hat{\varphi} + \omega t, \quad (1)$$

where \hat{e}_z is the basis vector associated with z , and $\hat{\varphi}$ the initial value of φ .

The wave fronts that are emitted by this point source in an empty and unbounded space are described by

$$|\mathbf{x}_P - \mathbf{x}(t)| = c(t_P - t), \quad (2)$$

where the constant c denotes the wave speed, and the coordinates $(\mathbf{x}_P, t_P) = (r_P, \varphi_P, z_P, t_P)$ mark the spacetime of observation points. The distance R between the observation point \mathbf{x}_P and a source point \mathbf{x} is given by

$$|\mathbf{x}_P - \mathbf{x}| \equiv R(\varphi) = [(z_P - z)^2 + r_P^2 + r^2 - 2r_P r \cos(\varphi_P - \varphi)]^{\frac{1}{2}}, \quad (3)$$

so that inserting (1) in (2) we obtain

$$R(t) \equiv [(z_P - z)^2 + r_P^2 + r^2 - 2r_P r \cos(\varphi_P - \hat{\varphi} - \omega t)]^{\frac{1}{2}} = c(t_P - t). \quad (4)$$

These wave fronts are expanding spheres of radii $c(t_P - t)$ whose fixed centres $(r_P = r, \varphi_P = \hat{\varphi} + \omega t, z_P = z)$ depend on their emission times t (see Fig. 1).

Introducing the natural length scale of the problem, c/ω , and using $t = (\varphi - \hat{\varphi})/\omega$ to eliminate t in favour of φ , we can express (4) in terms of dimensionless variables as

$$g \equiv \varphi - \varphi_P + \hat{R}(\varphi) = \phi, \quad (5)$$

in which $\hat{R} \equiv R\omega/c$, and

$$\phi \equiv \hat{\varphi} - \hat{\varphi}_P \quad (6)$$

stands for the difference between the positions $\hat{\varphi} = \varphi - \omega t$ of the source point and $\hat{\varphi}_P \equiv \varphi_P - \omega t_P$ of the observation point in the $(r, \hat{\varphi}, z)$ -space. The Lagrangian coordinate $\hat{\varphi}$ in (5) lies within an interval of length 2π (e.g. $-\pi < \hat{\varphi} \leq \pi$), while the angle φ , which denotes the azimuthal position of the source point at the retarded time t , ranges over $(-\infty, \infty)$.

Figure 1 depicts the wave fronts described by (5) for fixed values of $(r, \hat{\varphi}, z)$ and of ϕ (or t_P), and a discrete set of values of φ (or t). [In this

figure, the heavier curves show the cross section of the envelope with the plane of the orbit of the source. The larger of the two dotted circles designates the orbit (at $\tau = 3c/\omega$) and the smaller the light cylinder. ($\tau_P = c/\omega$).]

These wave fronts possess an envelope because when $\tau > c/\omega$, and so the speed of the source exceeds the wave speed, several wave fronts with differing emission times can pass through a single observation point simultaneously. Or stated mathematically, for certain values of the coordinates $(\tau_P, \varphi_P, z_P; \tau, z)$ the function $g(\varphi)$ shown in Fig. 2 is oscillatory and so can equal ϕ at more than one value of the retarded position φ : a horizontal line $\phi = \text{constant}$ intersects the curve (a) in Fig. 2 at either one or three points. [Fig. 2 is drawn for $\varphi_P = 0$, $\hat{r}_P = 3$, $\hat{r} = 2$ and (a) $\hat{z} = \hat{z}_P$, inside the envelope, (b) $\hat{z} = \hat{z}_c$, on the cusp curve of the envelope, (c) $\hat{z} = 2\hat{z}_c - \hat{z}_P$, outside the envelope. The marked adjacent turning points of curve (a) have the coordinates $(\varphi_{\pm}, \phi_{\pm})$, and φ_{out} represents the solution of $g(\varphi) = \phi_0$ for a ϕ_0 that tends to ϕ_- from below.]

Wave fronts become tangent to one another and so form an envelope at those points (τ_P, φ_P, z_P) for which two roots of $g(\varphi) = \phi$ coincide. The equation describing this envelope can therefore be obtained by eliminating φ between $g = \phi$ and $\partial g / \partial \varphi = 0$.

Thus, the values of φ on the envelope of the wave fronts are given by

$$\partial g / \partial \varphi = 1 - \hat{r} \hat{r}_P \sin(\varphi_P - \varphi) / \hat{R}(\varphi) = 0. \quad (7)$$

When the curve representing $g(\varphi)$ is as in Fig. 2(a) (i.e. $\hat{r} > 1$ and $\Delta > 0$), this equation has the doubly infinite set of solutions $\varphi = \varphi_{\pm} + 2n\pi$, where

$$\varphi_{\pm} = \varphi_P + 2\pi - \arccos[(1 \mp \Delta^{\frac{1}{2}}) / (\hat{r} \hat{r}_P)], \quad (8)$$

$$\Delta \equiv (\hat{r}_P^2 - 1)(\hat{r}^2 - 1) - (\hat{z} - \hat{z}_P)^2, \quad (9)$$

n is an integer, and $(\hat{r}, \hat{z}; \hat{r}_P, \hat{z}_P)$ stand for the dimensionless coordinates $\tau\omega/c$, $z\omega/c$, $\tau_P\omega/c$ and $z_P\omega/c$, respectively. The function $g(\varphi)$ is locally maximum at $\varphi_+ + 2n\pi$ and minimum at $\varphi_- + 2n\pi$.

Inserting $\varphi = \varphi_{\pm}$ in (5) and solving the resulting equation for ϕ as a function of (\hat{r}_P, \hat{z}_P) , we find that the envelope of the wave fronts is composed of two sheets:

$$\phi = \phi_{\pm} \equiv g(\varphi_{\pm}) = 2\pi - \arccos[(1 \mp \Delta^{\frac{1}{2}}) / (\hat{r} \hat{r}_P)] + \hat{R}_{\pm}, \quad (10)$$

in which

$$\hat{R}_{\pm} \equiv [(\hat{z} - \hat{z}_P)^2 + \hat{r}^2 + \hat{r}_P^2 - 2(1 \mp \Delta^{\frac{1}{2}})]^{\frac{1}{2}} \quad (11)$$

are the values of \hat{R} at $\varphi = \varphi_{\pm}$. For a fixed source point $(\tau, \hat{\varphi}, z)$, equation (10) describes a tube-like spiralling surface in the $(\tau_P, \hat{\varphi}_P, z_P)$ -space of observation points that extends from the speed-of-light cylinder $\hat{r}_P = 1$ to infinity. [A three-dimensional view of the light cylinder and the envelope of the wave fronts for the same source point (S) as that in Fig. 1 is presented in Fig. 3 (only those parts of these surfaces are shown which lie within the cylindrical volume $\hat{r}_P \leq 9$, $-2.25 \leq \hat{z}_P - \hat{z} \leq 2.25$).]

The two sheets $\phi = \phi_{\pm}$ of this envelope meet at a cusp. The cusp occurs along the curve

$$\phi = 2\pi - \arccos[1/(\hat{r}\hat{r}_P)] + (\hat{r}_P^2\hat{r}^2 - 1)^{\frac{1}{2}} \equiv \phi_c, \quad (12a)$$

$$\hat{z} = \hat{z}_P \pm (\hat{r}_P^2 - 1)^{\frac{1}{2}}(\hat{r}^2 - 1)^{\frac{1}{2}} \equiv \hat{z}_c, \quad (12b)$$

shown in Fig. 4 and constitutes the locus of points at which *three* different wave fronts intersect tangentially. [Figure 4 depicts the segment $-15 \leq \hat{z}_P - \hat{z} \leq 15$ of the cusp curve of the envelope shown in Fig. 3. This curve touches—and is tangent to—the light cylinder at the point $(\hat{r}_P = 1, \hat{z}_P = \hat{z}, \phi = \phi_c|_{\hat{r}_P=1})$ on the plane of the orbit.]

On the cusp curve $\phi = \phi_c$, $z = z_c$, the function $g(\varphi)$ has a point of inflection [Fig. 2(b)] and $\partial^2 g / \partial \varphi^2$, as well as $\partial g / \partial \varphi$ and g , vanish at

$$\varphi = \varphi_P + 2\pi - \arccos[1/(\hat{r}\hat{r}_P)] \equiv \varphi_c. \quad (12c)$$

This, in conjunction with $t = (\varphi - \hat{\varphi})/\omega$, represents the common emission time of the three wave fronts that are mutually tangential at the cusp curve of the envelope.

In the highly superluminal regime, where $\hat{r} \gg 1$, the separation of the ordinates ϕ_+ and ϕ_- of adjacent maxima and minima in Fig. 2(a) can be greater than 2π . A horizontal line $\phi = \text{constant}$ will then intersect the curve representing $g(\varphi)$ at more than three points, and so give rise to simultaneously received contributions that are made at 5, 7, ..., distinct values of the retarded time. In such cases, the sheet ϕ_- of the envelope (issuing from the conical apex of this surface) undergoes a number of intersections with the sheet ϕ_+ before reaching the cusp curve. We shall be concerned in this paper, however, mainly with source elements whose distances from the rotation axis do not appreciably exceed the radius c/ω of the speed-of-light cylinder and so for which the equation $g(\varphi) = \phi$ has at most three solutions.

At points of tangency of their fronts, the waves which interfere constructively to form the envelope propagate normal to the sheets $\phi = \phi_{\pm}(\tau_P, z_P)$ of this surface, in the directions

$$\begin{aligned} \hat{n}_{\pm} &\equiv (c/\omega) \nabla_P (\phi_{\pm} - \phi) \\ &= \hat{e}_{r_P} [\hat{r}_P - \hat{r}_P^{-1}(1 \mp \Delta^{\frac{1}{2}})] / \hat{R}_{\pm} + \hat{e}_{\varphi_P} / \hat{r}_P + \hat{e}_{z_P} (\hat{z}_P - \hat{z}) / \hat{R}_{\pm}, \end{aligned} \quad (13)$$

with the speed c . (\hat{e}_{r_P} , \hat{e}_{φ_P} and \hat{e}_{z_P} are the unit vectors associated with the cylindrical coordinates r_P , φ_P and z_P of the observation point, respectively.) Nevertheless, the resulting envelope is a rigidly rotating surface whose shape does not change with time: in the (r_P, φ_P, z_P) -space, its conical apex is stationary at (r, φ, z) , and its form and dimensions only depend on the constant parameter \hat{r} .

The set of waves that superpose coherently to form a particular section of the envelope or its cusp, therefore, cannot be the same (i.e. cannot have the same emission times) at different observation times. The packet of focused waves constituting any given segment of the cusp curve of the envelope, for instance, is constantly dispersed and reconstructed out of other waves. This one-dimensional caustic would not be unlimited in its extent, as shown in Fig. 4, unless the source is infinitely long-lived: only then would the duration of the source encompass the required intervals of emission time for every one of its constituent segments.

II. AMPLITUDES OF THE WAVES GENERATED BY A POINT SOURCE

Our discussion has been restricted so far to the geometrical features of the emitted wave fronts. In this section we proceed to find the Lienard-Wiechert potential for these waves.

The scalar potential arising from an element of the moving volume source we have been considering is given by the retarded solution of the wave equation

$$\nabla'^2 G_0 - \partial^2 G_0 / \partial (ct')^2 = -4\pi\rho_0, \quad (14a)$$

in which

$$\rho_0(r', \varphi', z', t') = \delta(r' - r)\delta(\varphi' - \omega t' - \varphi)\delta(z' - z)/r' \quad (14b)$$

is the density of a point source of unit strength with the trajectory (1). In the absence of boundaries, therefore, this potential has the value

$$G_0(x_P, t_P) = \int d^3x' dt' \rho_0(x', t') \delta(t_P - t' - |x_P - x'|/c) / |x_P - x'| \quad (15a)$$

$$= \int_{-\infty}^{+\infty} dt' \delta[t_P - t' - R(t')/c] / R(t'), \quad (15b)$$

where $R(t')$ is the function defined in (4) (see e.g. Jackson, *Classical Electrodynamics*, Wiley, New York 1975).

If we use (1) to change the integration variable t' in (15b) to φ , and express the resulting integrand in terms of the quantities introduced in (3), (5) and (6), we arrive at

$$G_0(\tau, \tau_P, \hat{\varphi} - \hat{\varphi}_P, z - z_P) = \int_{-\infty}^{+\infty} d\varphi \delta[g(\varphi) - \phi] / R(\varphi). \quad (16)$$

This can then be rewritten, by formally evaluating the integral, as

$$G_0 = \sum_{\varphi=\varphi_j} \frac{1}{R|\partial g/\partial \varphi|}, \quad (17)$$

where the angles φ_j are the solutions of the transcendental equation $g(\varphi) = \phi$ in $-\infty < \varphi < +\infty$ and correspond, in conjunction with (1), to the retarded times at which the source point $(\tau, \hat{\varphi}, z)$ makes its contribution towards the value of G_0 at the observation point $(\tau_P, \hat{\varphi}_P, z_P)$.

Equation (17) shows, in the light of Fig. 2, that the potential G_0 of a point source is discontinuous on the envelope of the wave fronts: if we approach the envelope from outside, the sum in (17) has only a single term and yields a finite value for G_0 , but if we approach this surface from inside, two of the φ_j s coalesce at an extremum of g and (17) yields a divergent value for G_0 . Approaching the sheet $\phi = \phi_+$ or $\phi = \phi_-$ of the envelope from inside this surface corresponds, in Fig. 2, to raising or lowering a horizontal line $\phi = \phi_0 = \text{const.}$, with $\phi_- \leq \phi_0 \leq \phi_+$, until it intersects the curve (a) of this figure at its maximum or minimum tangentially. At an observation point thus approached, the sum in (17) has three terms, two of which tend to infinity.

On the other hand, approaching a neighbouring observation point just outside the sheet $\phi = \phi_-$ (say) of the envelope corresponds, in Fig. 2, to raising a horizontal line $\phi = \phi_0 = \text{const.}$, with $\phi_0 \leq \phi_-$, towards a limiting position in which it tends to touch curve (a) at its minimum. So long as it has not yet reached the limit, such a line intersects curve (a) at one point only. The equation $g(\varphi) = \phi$ therefore has only a single solution $\varphi = \varphi_{\text{out}}$ in this case which is different from both φ_+ and φ_- and so at which $\partial g/\partial \varphi$ is non-zero (see Fig. 2). The contribution that the source makes when located at $\varphi = \varphi_{\text{out}}$ is received by both observers, but the constructively interfering waves that are emitted at the two retarded positions approaching φ_- only reach the observer inside the envelope.

The function G_0 has an even stronger singularity at the cusp curve of the envelope. On this curve, all three of the φ_j s coalesce [Fig. 2(b)] and each denominator in the expression in (17) both vanishes and has a vanishing derivative ($\partial g/\partial \varphi = \partial^2 g/\partial \varphi^2 = 0$).

There is a standard asymptotic technique for evaluating radiation integrals with coalescing critical points that describe caustics. By applying this technique—which we have outlined in Appendix A—to the integral in (16), we can obtain a uniform asymptotic approximation to G_0 for small $|\phi_+ - \phi_-|$, i.e. for points close to the cusp curve of the envelope where G_0 is most singular. The result is

$$G_0^{\text{in}} \sim 2c_1^{-2}(1 - \chi^2)^{-\frac{1}{2}} [p_0 \cos(\frac{1}{3} \arcsin \chi) - c_1 q_0 \sin(\frac{2}{3} \arcsin \chi)], \quad |\chi| < 1, \quad (18)$$

and

$$G_0^{\text{out}} \sim c_1^{-2}(\chi^2 - 1)^{-\frac{1}{2}} [p_0 \sinh(\frac{1}{3} \operatorname{arccosh} |\chi|) + c_1 q_0 \operatorname{sgn}(\chi) \sinh(\frac{2}{3} \operatorname{arccosh} |\chi|)], \quad |\chi| > 1, \quad (19)$$

where c_1 , p_0 , q_0 and χ are the functions of (τ, z) defined in (A2), (A5), (A6) and (A10), and approximated in (A23)–(A30). The superscripts 'in' and 'out' designate the values of G_0 inside and outside the envelope, and the variable χ equals $+1$ and -1 on the sheets $\phi = \phi_+$ and $\phi = \phi_-$ of this surface, respectively.

The function G_0^{out} is indeterminate but finite on the envelope [cf. (A39)], whereas G_0^{in} diverges like $\sqrt{3}c_1^{-2}(p_0 \mp c_1 q_0)/(1 - \chi^2)^{\frac{1}{2}}$ as $\chi \rightarrow \pm 1$. The singularity structure of G_0^{in} close to the cusp curve is explicitly exhibited by

$$G_0^{\text{in}} \sim \frac{2}{3^{\frac{1}{2}}} (\omega/c) (\hat{r}^2 \hat{r}_P^2 - 1)^{-\frac{1}{2}} c_0^{\frac{1}{2}} (\hat{z}_c - \hat{z})^{\frac{1}{2}} / [c_0^3 (\hat{z}_c - \hat{z})^3 - (\phi_c - \phi)^2]^{\frac{1}{2}}, \quad (20)$$

in which $0 \leq \hat{z}_c - \hat{z} \ll 1$, $|\phi_c - \phi| \ll 1$ and

$$c_0 \equiv \frac{2}{3^{\frac{1}{2}}} (\hat{r}^2 \hat{r}_P^2 - 1)^{-1} (\hat{r}_P^2 - 1)^{\frac{1}{2}} (\hat{r}^2 - 1)^{\frac{1}{2}} \quad (21)$$

[see (18) and (A22)–(A26)]. It can be seen from this expression that both the singularity on the envelope (at which the quantity inside the square brackets vanishes) and the singularity at the cusp curve (at which $\hat{z}_c - \hat{z}$ and $\phi_c - \phi$ vanish) are integrable singularities.

The potential of a volume source, which is given by the superposition of the potentials G_0 of its constituent volume elements, and so involves integrations with respect to $(\tau, \hat{\phi}, z)$, is therefore finite. Since they are created by the coordinated motion of aggregates of particles, the types of sources we have been considering cannot, of course, be point-like. It is only in the physically unrealizable case where a superluminal source is point-like that its potential has the extended singularities described above.

In fact, not only is the potential of an extended superluminally moving source singularity free, but it decays in the far zone like the potential of any other source. The following alternative form of the retarded solution to the wave equation $\nabla^2 A_0 - \partial^2 A_0 / \partial (ct)^2 = -4\pi\rho$ [which may be obtained from (15a) by performing the integration with respect to time]:

$$A_0 = \int d^3x \rho(\mathbf{x}, t_P - |\mathbf{x} - \mathbf{x}_P|/c) / |\mathbf{x} - \mathbf{x}_P| \quad (22)$$

shows that if the density ρ of the source is finite and vanishes outside a finite volume, then the potential A_0 decays like $|\mathbf{x}_P|^{-1}$ as the distance $|\mathbf{x}_P - \mathbf{x}| \simeq |\mathbf{x}_P|$ of the observer from the source tends to infinity.

III. THE BIFURCATION SURFACE OF AN OBSERVER

Let us now consider an *extended* source which rotates about the z -axis with the constant angular frequency ω . The density of such a source—when it has a distribution with an unchanging pattern—is given by

$$\rho(\tau, \varphi, z, t) = \rho(\tau, \hat{\varphi}, z), \quad (23)$$

where the Lagrangian variable $\hat{\varphi}$ is defined by $\varphi - \omega t$ as in (1), and ρ can be any function of $(\tau, \hat{\varphi}, z)$ that vanishes outside a finite volume.

If we insert this density in the expression for the retarded scalar potential and change the variables of integration from (τ, φ, z, t) to $(\tau, \hat{\varphi}, z, t)$, we obtain

$$A_0(\mathbf{x}_P, t_P) = \int d^3x dt \rho(\mathbf{x}, t) \delta(t_P - t - |\mathbf{x} - \mathbf{x}_P|/c) / |\mathbf{x} - \mathbf{x}_P| \quad (24a)$$

$$= \int \tau d\tau d\hat{\varphi} dz \rho(\tau, \hat{\varphi}, z) G_0(\tau, \tau_P, \hat{\varphi} - \hat{\varphi}_P, z - z_P), \quad (24b)$$

where G_0 is the function defined in (16) which represents the scalar potential of a corresponding point source. That the potential of the extended source in question is given by the superposition of the potentials of the moving source points that constitute it is an advantage that is gained by marking the space of source points with the natural coordinates $(\tau, \hat{\varphi}, z)$ of the source distribution. This advantage is lost if we use any other coordinates.

In Sec. II, where the source was point-like, the coordinates $(\tau, \hat{\varphi}, z)$ of the source point in $G_0(\tau, \tau_P, \hat{\varphi} - \hat{\varphi}_P, z - z_P)$ were held fixed and we were concerned with the behaviour of this potential as a function of the coordinates $(\tau_P, \hat{\varphi}_P, z_P)$ of the observation point. When we superpose the potentials of

the volume elements that constitute an extended source, on the other hand, the coordinates (τ_P, ϕ_P, z_P) are held fixed and we are primarily concerned with the behaviour of G_0 as a function of the integration variables (τ, ϕ, z) .

Because G_0 is invariant under the interchange of (τ, ϕ, z) and (τ_P, ϕ_P, z_P) if ϕ is at the same time changed to $-\phi$ [see (5) and (16)], the singularity of G_0 occurs on a surface in the (τ, ϕ, z) -space of source points which has the same shape as the envelope shown in Fig. 3 but issues from the fixed point (τ_P, ϕ_P, z_P) and spirals around the z -axis in the opposite direction to the envelope. [See Fig. 5 in which the light cylinder and the bifurcation surface associated with the observation point P are shown for a counterclockwise source motion. In this figure, P is located at $\hat{r}_P = 9$, and only those parts of these surfaces are shown which lie within the cylindrical volume $\hat{r} \leq 11$, $-1.5 \leq z - \hat{z}_P \leq 1.5$. The two sheets $\phi = \phi_{\pm}(\tau, z)$ of the bifurcation surface meet along a cusp (a curve of the same shape as that shown in Fig. 4) that is tangent to the light cylinder. For an observation point in the far zone ($\hat{r}_P \gg 1$), the spiralling surface that issues from P undergoes a large number of turns—in which its two sheets intersect one another—before reaching the light cylinder.]

In this paper, we refer to this locus of singularities of G_0 as the *bifurcation surface* of the observation point P .

Consider an observation point P for which the bifurcation surface intersects the source distribution, as in Fig. 6. [In Fig. 6, the full curves depict the cross section, with the cylinder $\hat{r} = 1.5$, of the bifurcation surface of an observer located at $\hat{r}_P = 3$. (The motion of the source is counterclockwise.) Projection of the cusp curve of this bifurcation surface onto the cylinder $\hat{r} = 1.5$ is shown as a dotted curve, and the region occupied by the source as a dotted area. In this figure the observer's position is such that one of the points $(\phi = \phi_c, z = z_c)$ at which the cusp curve in question intersects the cylinder $\hat{r} = 1.5$ —the one with $z_c > 0$ —is located within the source distribution. As the radial position τ_P of the observation point tends to infinity, the separation—at a finite distance $z_c - z$ from (ϕ_c, z_c) —of the shown cross sections decreases like $\tau_P^{-\frac{1}{2}}$.]

The envelope of the wave fronts emanating from a volume element of the part of the source that lies within this bifurcation surface encloses the point P , but P is exterior to the envelope associated with a source element that lies outside the bifurcation surface.

We have seen that three wave fronts—propagating in different directions—simultaneously pass an observer who is located inside the envelope of the waves emanating from a point source, and only one wavefront passes an observer outside this surface. Hence, in contrast to the source elements outside the bifurcation surface which influence the potential at P at only a single

value of the retarded time, this potential receives contributions from each of the elements inside the bifurcation surface at *three* distinct values of the retarded time.

The elements inside but adjacent to the bifurcation surface, for which G_0 diverges, are sources of the constructively interfering waves that not only arrive at P simultaneously but also are emitted at the same (retarded) time. These source elements approach the observer along the radiation direction $x_P - x$ with the wave speed at the retarded time, i.e. are located at distances $R(t)$ from the observer for which

$$\left. \frac{dR}{dt} \right|_{t=t_P - R/c} = -c \quad (25)$$

[see (4), (7) and (8)]. Their accelerations at the retarded time,

$$\left. \frac{d^2 R}{dt^2} \right|_{t=t_P - R/c} = \mp \frac{c\omega \Delta^{\frac{1}{2}}}{\bar{R}_{\pm}}, \quad (26)$$

are positive on the sheet $\phi = \phi_-$ of the bifurcation surface and negative on $\phi = \phi_+$.

The source points on the *cusp curve* of the bifurcation surface, for which $\Delta = 0$ and all three of the contributing retarded times coincide, approach the observer—according to (26)—with zero acceleration as well as with the wave speed.

From a radiative point of view, the most effective volume elements of the superluminal source in question are those that approach the observer along the radiation direction with the wave speed and zero acceleration at the retarded time, since the ratio of the emission to reception time intervals for the waves that are generated by these particular source elements generally exceeds unity by several orders of magnitude. On each constituent ring of the source distribution that lies outside the light cylinder ($r = c/\omega$) in a plane of rotation containing the observation point, there are two volume elements that approach the observer with the wave speed at the retarded time: one whose distance from the observer diminishes with positive acceleration, and another for which this acceleration is negative. These two elements are closer to one another the smaller the radius of the ring. For the smallest of such constituent rings, i.e. for the one that lies on the light cylinder, the two volume elements in question coincide and approach the observer also with zero acceleration.

The other constituent rings of the source distribution (those on the planes of rotation which do not pass through the observation point) likewise

contain two such elements if their radii are large enough for their velocity $\tau\omega e_\phi$ to have a component along the radiation direction equal to c . On the smallest possible ring in each plane, there is again a single volume element—at the limiting position of the two coalescing volume elements of the neighbouring larger rings—that moves towards the observer not only with the wave speed but also with zero acceleration.

For any given observation point P , the efficiently radiating pairs of volume elements on various constituent rings of the source distribution collectively form a surface: the part of the bifurcation surface associated with P which intersects the source distribution. The locus of the coincident pairs of volume elements, which is tangent to the light cylinder at the point where it crosses the plane of rotation containing the observer, constitutes the segment of the cusp curve of this bifurcation surface that lies within the source distribution.

Thus the bifurcation surface associated with any given observation point divides the volume of the source into two sets of elements with differing influences on the observed field. As in (18) and (19), the potentials G_0^{in} and G_0^{out} of the source elements inside and outside the bifurcation surface have different forms: the boundary $|\chi(\tau, \tau_P, \hat{\phi} - \hat{\phi}_P, z - z_P)| = 1$ between the domains of validity of (18) and (19) delineates the envelope of wave fronts when the source point $(\tau, \hat{\phi}, z)$ is fixed and the coordinates $(\tau_P, \hat{\phi}_P, z_P)$ of the observation point are variable, and describes the bifurcation surface when the observation point $(\tau_P, \hat{\phi}_P, z_P)$ is fixed and the coordinates $(\tau, \hat{\phi}, z)$ of the source point sweep a volume.

The expression (24b) for the scalar potential correspondingly splits into the following two terms when the observation point is such that the bifurcation surface intersects the source distribution:

$$A_0 = \int dV \rho G_0 \quad (27a)$$

$$= \int_{V_{\text{in}}} dV \rho G_0^{\text{in}} + \int_{V_{\text{out}}} dV \rho G_0^{\text{out}}, \quad (27b)$$

where $dV \equiv r dr d\hat{\phi} dz$, V_{in} and V_{out} designate the portions of the source which fall inside and outside the bifurcation surface (see Fig. 6), and G_0^{in} and G_0^{out} denote the different expressions for G_0 in these two regions.

Note that the boundaries of the volume V_{in} depend on the position $(\tau_P, \hat{\phi}_P, z_P)$ of the observer: the parameter \hat{r}_P fixes the shape and size of the bifurcation surface, and the position $(\tau_P, \hat{\phi}_P, z_P)$ of the observer specifies the location of the conical apex of this surface. When the observation point is such that the cusp curve of the bifurcation surface intersects the source distribution, the volume V_{in} is bounded by $\phi = \phi_-$, $\phi = \phi_+$, and the part of

the source boundary $\rho(\tau, \hat{\phi}, \hat{z}) = 0$ that falls within the bifurcation surface. The corresponding volume V_{out} is bounded by the same patches of the two sheets of the bifurcation surface and by the remainder of the source boundary.

In the vicinity of the cusp curve (12), i.e. for $|\phi_c - \phi| \ll 1$ and $0 \leq \hat{z}_c - \hat{z} \ll 1$, the cross section of the bifurcation surface with a cylinder $\hat{r} = \text{constant}$ is described by

$$\begin{aligned} \phi_{\pm} - \phi_c &\simeq -(\hat{r}^2 - 1)^{\frac{1}{2}}(\hat{r}_P^2 - 1)^{\frac{1}{2}}(\hat{r}^2 \hat{r}_P^2 - 1)^{-\frac{1}{2}}(\hat{z}_c - \hat{z}) \\ &\pm \frac{2^{\frac{3}{2}}}{3}(\hat{r}^2 - 1)^{\frac{3}{2}}(\hat{r}_P^2 - 1)^{\frac{3}{2}}(\hat{r}_P^2 \hat{r}^2 - 1)^{-\frac{3}{2}}(\hat{z}_c - \hat{z})^{\frac{3}{2}} \end{aligned} \quad (28)$$

[see (10)–(12) and (A26)]. This cross section, which is shown in Fig. 6, has two branches meeting at the intersections of the cusp curve with the cylinder $\hat{r} = \text{constant}$ whose separation in ϕ —at a given $(\hat{z}_c - \hat{z})$ —diminishes like $\hat{r}_P^{-\frac{3}{2}}$ in the limit $\hat{r}_P \rightarrow \infty$. Thus, at finite distances $\hat{z}_c - \hat{z}$ from the cusp curve, the two sheets $\phi = \phi_-$ and $\phi = \phi_+$ of the bifurcation surface coalesce and become coincident with the surface $\phi = \frac{1}{2}(\phi_- + \phi_+) \equiv c_2$ as $\hat{r}_P \rightarrow \infty$. That is to say, the volume V_{in} vanishes like $\hat{r}_P^{-\frac{3}{2}}$.

Because the dominant contributions towards the value of the radiation field come from those source elements that approach the observer—along the radiation direction—with the wave speed and zero acceleration at the retarded time, in what follows, we shall be primarily interested in far-field observers the cusp curves of whose bifurcation surfaces intersect the source distribution. For such observers, the Green's function $\lim_{\hat{r}_P \rightarrow \infty} G_0$ undergoes a jump discontinuity across the coalescing sheets of the bifurcation surface: the values of χ on the sheets $\phi = \phi_{\pm}$, and hence the functions $G_0^{\text{out}}|_{\phi=\phi_-}$ and $G_0^{\text{out}}|_{\phi=\phi_+}$, remain different even in the limit where $\phi = \phi_-$ and $\phi = \phi_+$ coincide [cf. (A10) and (A39)].

IV. DERIVATIVES OF THE RADIATION INTEGRALS AND THEIR HADAMARD'S FINITE PARTS

A. Gradient of the scalar potential

In this section we begin the calculation of the electric and magnetic fields by finding the gradient of the scalar potential A_0 , i.e. by calculating the derivatives of the integral in (27a) with respect to the coordinates (τ_P, φ_P, z_P) of the observation point.

If we regard its singular kernel G_0 as a classical function, then the integral in (27a) is improper and cannot be differentiated under the integral sign without characterizing and duly handling the singularities of its integrand. On the other hand, if we regard G_0 as a generalized function, then it would

be mathematically permissible to interchange the orders of differentiation and integration when calculating $\nabla_P A_0$.

This interchange results in a new kernel $\nabla_P G_0$ whose singularities are non-integrable. However, the theory of generalized functions prescribes a well-defined procedure for obtaining the physically relevant value of the resulting divergent integral, a procedure involving integration by parts which extracts the so-called Hadamard's finite part of this integral (see e.g. Hoskins, *Generalised Functions*, Ellis Horwood, London 1979). Hadamard's finite part of the divergent integral representing $\nabla_P A_0$ yields the value that we would have obtained if we had first evaluated the original integral for A_0 as an explicit function of (r_P, ϕ_P, z_P) and then differentiated it.

From the standpoint of the theory of generalized functions, therefore, differentiation of (27a) yields

$$\nabla_P A_0 = \int dV \rho \nabla_P G_0 = (\nabla_P A_0)_{\text{in}} + (\nabla_P A_0)_{\text{out}}, \quad (29a)$$

in which

$$(\nabla_P A_0)_{\text{in,out}} \equiv \int_{V_{\text{in,out}}} dV \rho \nabla_P G_0^{\text{in,out}}. \quad (29b)$$

Since ρ vanishes outside a finite volume, the integral in (27a) extends over all values of (r, ϕ, z) and so there is no contribution from the limits of integration towards the derivative of this integral.

The kernels $\nabla_P G_0^{\text{in,out}}$ of the above integrals may be obtained from (16). Applying ∇_P to the right-hand side of (16) and interchanging the orders of differentiation and integration, we obtain an integral representation of $\nabla_P G_0$ consisting of two terms: one arising from the differentiation of R which decays like r_P^{-2} as $r_P \rightarrow \infty$ and so makes no contribution to the field in the radiation zone, and another that arises from the differentiation of the Dirac delta function and decays less rapidly than r_P^{-2} . For an observation point in the radiation zone, we may discard terms of the order of r_P^{-2} and write

$$\nabla_P G_0 \simeq (\omega/c) \int_{-\infty}^{+\infty} d\phi R^{-1} \delta'(g - \phi) \hat{n}, \quad \hat{r}_P \gg 1, \quad (30)$$

in which δ' is the derivative of the Dirac delta function with respect to its argument and

$$\hat{n} \equiv \hat{e}_{r_P} [\hat{r}_P - \hat{r} \cos(\phi - \phi_P)] / \hat{R} + \hat{e}_{\phi_P} / \hat{r}_P + \hat{e}_{z_P} (\hat{z}_P - \hat{z}) / \hat{R}. \quad (31)$$

Equation (30) yields $\nabla_P G_0^{\text{in}}$ or $\nabla_P G_0^{\text{out}}$ depending on whether ϕ lies within the interval (ϕ_-, ϕ_+) or outside it.

If we now insert (30) in (29b) and perform the integrations with respect to ϕ by parts, we find that

$$(\nabla_P A_0)_{\text{in}} \simeq (\omega/c) \int_S r dr dz \left\{ -[\rho G_1^{\text{in}}]_{\phi=\phi_-}^{\phi=\phi_+} + \int_{\phi_-}^{\phi_+} d\phi \partial \rho / \partial \phi G_1^{\text{in}} \right\}, \quad \hat{r}_P \gg 1, \quad (32)$$

and

$$(\nabla_P A_0)_{\text{out}} \simeq (\omega/c) \int_S r dr dz \left\{ [\rho G_1^{\text{out}}]_{\phi=\phi_-}^{\phi=\phi_+} + \left(\int_{-\pi}^{\phi_-} + \int_{\phi_+}^{+\pi} \right) d\phi \partial \rho / \partial \phi G_1^{\text{out}} \right\}, \quad \hat{r}_P \gg 1, \quad (33)$$

in which S stands for the projection of V_{in} onto the (r, z) -plane, and G_1^{in} and G_1^{out} are given by the values of

$$G_1 \equiv \int_{-\infty}^{+\infty} d\varphi R^{-1} \delta(g - \phi) \hat{n} = \sum_{\varphi=\varphi_j} R^{-1} |\partial g / \partial \varphi|^{-1} \hat{n} \quad (34)$$

for ϕ inside and outside the interval (ϕ_-, ϕ_+) , respectively.

Like G_0^{in} , the Green's function G_1^{in} diverges on the bifurcation surface $\phi = \phi_{\pm}$, where $\partial g / \partial \varphi$ vanishes, but this singularity of G_0^{in} is integrable so that the value of the second integral in (32) is finite (see Sec. II and Appendix A). Hadamard's finite part of $(\nabla_P A_0)_{\text{in}}$ (denoted by the prefix Fp) is obtained by simply discarding those 'integrated' or boundary terms in (32) which diverge. Hence, the physically relevant quantity $\text{Fp}\{(\nabla_P A_0)_{\text{in}}\}$ consists—in the far zone—of the volume integral in (32).

Let us choose an observation point for which the cusp curve of the bifurcation surface intersects the source distribution (see Fig. 6). When the dimensions ($\sim L$) of the source are negligibly smaller than those of the bifurcation surface (i.e. when $L \ll r_P$ and so $z_c - z \ll r_P$ throughout the source distribution) the functions $G_1^{\text{in, out}}$ in (32) and (33) can be approximated by their asymptotic values (A34) and (A35) in the vicinity of the cusp curve (see Appendix A).

According to (A34), (A36) and (A44), G_1^{in} decays like $p_1/c_1^2 = O(1)$ at points interior to the bifurcation surface where $\lim_{R_P \rightarrow \infty} \chi$ remains finite. Since the separation of the two sheets of the bifurcation surface diminishes like $\hat{r}_P^{-\frac{3}{2}}$ within the source [see (28)], it therefore follows that the volume integral in (32) is of the order of $1 \times \hat{r}_P^{-\frac{3}{2}}$, a result which can also be inferred from the far-field version of (A34) by explicit integration. Hence,

$$\text{Fp}\{(\nabla_P A_0)_{\text{in}}\} = O(\hat{r}_P^{-\frac{3}{2}}), \quad \hat{r}_P \gg 1, \quad (35)$$

decays too rapidly to make any contribution towards the value of the electric field in the radiation zone.

Because G_1^{out} is, in contrast to G_1^{in} , finite on the bifurcation surface, both the surface and the volume integrals on the right-hand side of (33) have finite values. Each component of the second term has the same structure as the expression for the potential itself and so decays like r_P^{-1} (see the ultimate paragraph of Sec. II). But the first term—which would have cancelled the corresponding boundary term in (32) and so would not have survived in the expression for $\nabla_P A_0$ had the Green's function G_1 been continuous—behaves differently from any conventional contribution to a radiation field.

Insertion of (A39) in (33) yields the following expression for the asymptotic value of this boundary term in the limit where the observer is located in the far zone and the source is localized about the cusp curve of his (her) bifurcation surface:

$$\int r dr dz \left[\rho G_1^{\text{out}} \right]_{\phi_-}^{\phi_+} \sim \frac{1}{3} c_1^{-2} \int r dr dz \left[p_1(\rho|_{\phi_+} - \rho|_{\phi_-}) + 2c_1 q_1(\rho|_{\phi_+} + \rho|_{\phi_-}) \right]. \quad (36)$$

In this limit, the two sheets of the bifurcation surface are essentially coincident throughout the domain of integration in (36) [see (28)]. So the difference between the values of the source density on these two sheets of the bifurcation surface is negligibly small ($\sim \hat{r}_P^{-\frac{3}{2}}$) for a smoothly distributed source and the functions $\rho|_{\phi_{\pm}}$ appearing in the integrand of (36) may correspondingly be approximated by their common limiting value $\rho_{bs}(\tau, z)$ on these coalescing sheets.

Once the functions $\rho|_{\phi_{\pm}}$ are approximated by $\rho_{bs}(\tau, z)$ and q_1 by (A41), equation (36) yields an expression which can be written, to within the leading order in the far-field approximation $\hat{r}_P \gg 1$ [see (A44) and (A45)], as

$$\begin{aligned} \int_S r dr dz \left[\rho G_1^{\text{out}} \right]_{\phi_-}^{\phi_+} &\sim 2^{\frac{3}{2}} (c/\omega)^2 \hat{r}_P^{-\frac{3}{2}} \int_{\hat{r}_<}^{\hat{r}_>} d\hat{r} (\hat{r}^2 - 1)^{-\frac{1}{2}} \mathbf{n}_1 \\ &\quad \times \int_{\hat{z}_c - L_z \omega/c}^{\hat{z}_c} d\hat{z} (\hat{z}_c - \hat{z})^{-\frac{1}{2}} \rho_{bs}(\tau, z) \\ &\sim 2^{\frac{3}{2}} (c/\omega)^2 \hat{r}_P^{-\frac{3}{2}} \int_{\hat{r}_<}^{\hat{r}_>} d\hat{r} (\hat{r}^2 - 1)^{-\frac{1}{2}} \mathbf{n}_1 (L_z \omega/c)^{\frac{1}{2}} \langle \rho_{bs} \rangle, \end{aligned} \quad (37)$$

with

$$\langle \rho_{bs} \rangle(\tau) \equiv \int_0^1 d\eta \rho_{bs}(\tau, z) \Big|_{z=z_c - \eta^2 L_z}, \quad (38)$$

where $z_c - L_z(\tau) \leq z \leq z_c$ and $\tau_< \leq \tau \leq \tau_>$ are the intervals over which the bifurcation surface intersects the source distribution (see Fig. 6). The

quantity $\langle \rho_{bs} \rangle(\tau)$ may be interpreted, at any given τ , as a weighted average—over the intersection of the coalescing sheets of the bifurcation surface with the plane $z = z_c - \eta^2 L_z$ —of the source density ρ .

The right-hand side of (37) decays like $\tau_P^{-\frac{3}{2}}$ as $\tau_P \rightarrow \infty$. The second term in (33) thus dominates the first term in this equation, and so the quantity $(\nabla_P A_0)_{out}$ itself decays like τ_P^{-1} in the far zone.

B. Time derivative of the vector potential

Inasmuch as the charge density (23) has an unchanging distribution pattern in the $(\tau, \hat{\varphi}, z)$ -frame, the electric current density associated with the moving source we have been considering is given by

$$\mathbf{j}(\mathbf{x}, t) = \tau \omega \rho(\tau, \hat{\varphi}, z) \hat{\mathbf{e}}_\varphi, \quad (39)$$

in which $\tau \omega \hat{\mathbf{e}}_\varphi = \tau \omega [-\sin(\varphi - \varphi_P) \hat{\mathbf{e}}_{\tau_P} + \cos(\varphi - \varphi_P) \hat{\mathbf{e}}_{\varphi_P}]$ is the velocity of the element of the source pattern that is located at (τ, φ, z) . This current satisfies the continuity equation $\partial \rho / \partial(\tau) + \nabla \cdot \mathbf{j} = 0$ automatically.

In the Lorentz gauge, the retarded vector potential corresponding to (24a) has the form

$$\mathbf{A}(\mathbf{x}_P, t_P) = c^{-1} \int d^3x dt \mathbf{j}(\mathbf{x}, t) \delta(t_P - t - |\mathbf{x} - \mathbf{x}_P|/c) / |\mathbf{x} - \mathbf{x}_P|. \quad (40)$$

If we insert (39) in (40) and change the variables of integration from (τ, φ, z, t) to $(\tau, \varphi, z, \hat{\varphi})$, as in (24), we obtain

$$\mathbf{A} = \int dV \hat{\mathbf{r}} \rho(\tau, \hat{\varphi}, z) \mathbf{G}_2(\tau, \tau_P, \hat{\varphi} - \hat{\varphi}_P, z - z_P), \quad (41)$$

in which $dV = r dr d\hat{\varphi} dz$, the vector \mathbf{G}_2 —which plays the role of a Green's function—is given by

$$\mathbf{G}_2 \equiv \int_{-\infty}^{+\infty} d\varphi \hat{\mathbf{e}}_\varphi \delta[g(\varphi) - \phi] / R(\varphi) = \sum_{\varphi=\varphi_j} R^{-1} |\partial g / \partial \varphi|^{-1} \hat{\mathbf{e}}_\varphi, \quad (42)$$

and g and φ_j s are the same quantities as those appearing in (17) (see also Fig. 2).

Because (17), (34) and (42) have the factor $|\partial g / \partial \varphi|^{-1}$ in common, the function \mathbf{G}_2 has the same singularity structure as those of \mathbf{G}_0 and \mathbf{G}_1 : it diverges on the bifurcation surface $\partial g / \partial \varphi = 0$ if this surface is approached from inside, and it is most singular on the cusp curve of the bifurcation surface

where in addition $\partial^2 g / \partial \varphi^2 = 0$. It is, moreover, described by two different expressions, G_2^{in} and G_2^{out} , inside and outside the bifurcation surface whose asymptotic values in the neighbourhood of the cusp curve have exactly the same functional forms as those found in (18) and (19); the only difference being that p_0 and q_0 in these expressions are replaced by the p_2 and q_2 given in (A37) (see Appendix A).

As in (29), therefore, the time derivative of the vector potential has the form $\partial A / \partial t_P = (\partial A / \partial t_P)_{\text{in}} + (\partial A / \partial t_P)_{\text{out}}$ with

$$(\partial A / \partial t_P)_{\text{in,out}} \equiv -\omega \int_{V_{\text{in,out}}} dV \hat{r} \rho \partial G_2^{\text{in,out}} / \partial \hat{\varphi}_P \quad (43)$$

when the observation point is such that the bifurcation surface intersects the source distribution.

The functions $G_2^{\text{in,out}}$ depend on $\hat{\varphi}_P$ and $\hat{\varphi}$ in the combination $\hat{\varphi} - \hat{\varphi}_P$ only. We can therefore replace $\partial / \partial \hat{\varphi}_P$ in (43) by $-\partial / \partial \hat{\varphi}$ and perform the integration with respect to $\hat{\varphi}$ by parts to arrive at

$$(\partial A / \partial t_P)_{\text{in}} = c \int_S dr dz \hat{r}^2 \left\{ \left[\rho G_2^{\text{in}} \right]_{\hat{\varphi}=\hat{\varphi}_-}^{\hat{\varphi}=\hat{\varphi}_+} - \int_{\hat{\varphi}_-}^{\hat{\varphi}_+} d\hat{\varphi} \partial \rho / \partial \hat{\varphi} G_2^{\text{in}} \right\}, \quad (44)$$

and

$$\begin{aligned} (\partial A / \partial t_P)_{\text{out}} = & -c \int_S dr dz \hat{r}^2 \left\{ \left[\rho G_2^{\text{out}} \right]_{\hat{\varphi}=\hat{\varphi}_-}^{\hat{\varphi}=\hat{\varphi}_+} \right. \\ & \left. + \left(\int_{-\pi}^{\hat{\varphi}_-} + \int_{\hat{\varphi}_+}^{+\pi} \right) d\hat{\varphi} \partial \rho / \partial \hat{\varphi} G_2^{\text{out}} \right\}. \end{aligned} \quad (45)$$

For the same reasons as those given in the paragraphs following (32) and (33), Hadamard's finite part of $(\partial A / \partial t_P)_{\text{in}}$ consists of the volume integral in (44) and is of the order of $\hat{r}_P^{-\frac{3}{2}}$ [note that according to (A37) and (A42), $p_2 \gg c_1 q_2$ and $p_2 / c_1^2 = O(1)$]. The volume integral in (45), moreover, decays like \hat{r}_P^{-1} , as does its counterpart in (33).

The part of $\partial A / \partial t_P$ that decays more slowly than conventional contributions to a radiation field is the boundary term in (45). The asymptotic value of this term is given by an expression similar to that appearing in (36), except that p_1 and q_1 are replaced by p_2 and q_2 . Once the quantities $\rho|_{\hat{\varphi}_{\pm}}$ and q_2 in the expression in question are approximated by ρ_{bs} and by (A42), as before, it follows that

$$\begin{aligned} (\partial A / \partial t_P)_{\text{out}} & \sim -c \int_S dr dz \hat{r}^2 \left[\rho G_2^{\text{out}} \right]_{\hat{\varphi}_-}^{\hat{\varphi}_+} \sim -\frac{4}{3} c \int_S dr dz \hat{r}^2 \rho_{\text{bs}} c_1^{-1} q_2 \\ & \sim -\frac{2}{3} (c^2 / \omega) \hat{r}_P^{-\frac{1}{2}} \hat{e}_{\varphi_P} \int_{\hat{r}_c}^{\hat{r}} d\hat{r} \hat{r}^2 (\hat{r}^2 - 1)^{-\frac{1}{2}} \int_{\hat{z}_c - L_{\text{f}\omega/c}}^{\hat{z}_c} d\hat{z} (\hat{z}_c - \hat{z})^{-\frac{1}{2}} \rho_{\text{bs}} \end{aligned} \quad (46)$$

This behaves like $\hat{r}_P^{-\frac{1}{2}}$ as $\hat{r}_P \rightarrow \infty$ since the \hat{z} -quadrature in (46) has the finite value $2(L_z\omega/c)^{\frac{1}{2}}\langle\rho_{bs}\rangle$ in this limit [see (37) *et seq.*].

Hence, the electric field vector of the radiation

$$\begin{aligned} \mathbf{E} &= -\nabla_P A_0 - \partial\mathbf{A}/\partial(ct_P) \sim -c^{-1}(\partial\mathbf{A}/\partial t_P)_{\text{out}} \\ &\sim \frac{2^{\frac{1}{2}}}{3}(c/\omega)\hat{r}_P^{-\frac{1}{2}}\hat{\mathbf{e}}_{\varphi_P} \int_{\hat{r}_<}^{\hat{r}_>} d\hat{r}\hat{r}^2(\hat{r}^2-1)^{-\frac{1}{2}}(L_z\omega/c)^{\frac{1}{2}}\langle\rho_{bs}\rangle \end{aligned} \quad (47)$$

itself decays like $\tau_P^{-\frac{1}{2}}$ in the far zone: as we have already seen in Sec. IV(A), the term $\nabla_P A_0$ has the conventional rate of decay τ_P^{-1} and so is negligible relative to $(\partial\mathbf{A}/\partial t_P)_{\text{out}}$.

C. Curl of the vector potential

There are no contributions from the limits of integration towards the curl of the integral in (41) because ρ vanishes outside a finite volume and so the integral in this equation extends over all values of $(\tau, \hat{\varphi}, z)$. Hence, differentiation of (41) yields

$$\mathbf{B} = \nabla_P \times \mathbf{A} = \mathbf{B}_{\text{in}} + \mathbf{B}_{\text{out}}, \quad (48a)$$

in which

$$\mathbf{B}_{\text{in,out}} \equiv \int_{V_{\text{in,out}}} dV \hat{r} \rho \nabla_P \times \mathbf{G}_2^{\text{in,out}}. \quad (48b)$$

Operating with $\nabla_P \times$ on the first member of (42) and ignoring the term that decays like τ_P^{-2} , as in (30), we find that the kernels $\nabla_P \times \mathbf{G}_2^{\text{in}}$ and $\nabla_P \times \mathbf{G}_2^{\text{out}}$ of (48b) are given—in the radiation zone—by the values of

$$\nabla_P \times \mathbf{G}_2 \simeq (\omega/c) \int_{-\infty}^{+\infty} d\varphi R^{-1} \delta'(g - \phi) \hat{\mathbf{n}} \times \hat{\mathbf{e}}_{\varphi}, \quad \hat{r}_P \gg 1, \quad (49)$$

for ϕ inside and outside the interval (ϕ_-, ϕ_+) , respectively. [$\hat{\mathbf{n}}$ is the unit vector defined in (31).]

Insertion of (49) in (48) now yields expressions whose $\hat{\varphi}$ -quadratures can be evaluated by parts to arrive at

$$\mathbf{B}_{\text{in}} \simeq \int_S d\tau dz \hat{r}^2 \left\{ - \left[\rho \mathbf{G}_3^{\text{in}} \right]_{\phi=\phi_-}^{\phi=\phi_+} + \int_{\phi_-}^{\phi_+} d\phi \partial\rho/\partial\hat{\varphi} \mathbf{G}_3^{\text{in}} \right\}, \quad \hat{r}_P \gg 1, \quad (50)$$

and

$$\begin{aligned} \mathbf{B}_{\text{out}} \simeq \int_S d\tau dz \hat{r}^2 \left\{ \left[\rho \mathbf{G}_3^{\text{out}} \right]_{\phi=\phi_-}^{\phi=\phi_+} \right. \\ \left. + \left(\int_{-\pi}^{\phi_-} + \int_{\phi_+}^{+\pi} \right) d\phi \partial\rho/\partial\hat{\varphi} \mathbf{G}_3^{\text{out}} \right\}, \quad \hat{r}_P \gg 1, \quad (51) \end{aligned}$$

where G_3^{in} and G_3^{out} stand for the values of

$$G_3 \equiv \int_{-\infty}^{+\infty} d\varphi R^{-1} \delta(g - \phi) \hat{n} \times \hat{e}_\varphi = \sum_{\varphi=\varphi_j} R^{-1} |\partial g / \partial \varphi|^{-1} \hat{n} \times \hat{e}_\varphi \quad (52)$$

inside and outside the bifurcation surface.

Once again, owing to the presence of the factor $|\partial g / \partial \varphi|^{-1}$ in G_3^{in} , the first term in (50) is divergent so that the Hadamard's finite part of B_{in} consists of the volume integral in this equation, an integral whose magnitude is of the order of $\hat{r}_P^{-\frac{3}{2}}$ [see the paragraph containing (35) and note that, according to (A38) and (A44), $p_3 \gg c_1 q_3$ and $p_3 / c_1^2 = O(1)$]. The second term in (51) has—like those in (33) and (45)—the conventional rate of decay \hat{r}_P^{-1} . Moreover, the surface integral in (51)—which would have had the same magnitude as the surface integral in (50) and so would have cancelled out of the expression for B had G_3^{in} and G_3^{out} matched smoothly across the bifurcation surface—decays as slowly as the corresponding term in (45).

The asymptotic value of G_3 for source points close to the cusp curve of the bifurcation surface has been calculated in Appendix A. It follows from this value of G_3 and from (51), (52), (A40), (A44) and (A45) that, in the radiation zone,

$$\begin{aligned} B &\sim \int_S dr dz \hat{r}^2 \left[\rho G_3^{\text{out}} \right]_{\phi_-}^{\phi_+} \sim \frac{4}{3} \int_S dr dz \hat{r}^2 \rho_{\text{bs}} c_1^{-1} q_3 \\ &\sim \frac{2}{3} (c/\omega) \hat{r}_P^{-\frac{1}{2}} \int_{\hat{r}_c}^{\hat{r}} d\hat{r} \hat{r}^2 (\hat{r}^2 - 1)^{-\frac{1}{2}} \int_{\hat{z}_c - L_{\text{E}} \omega / c}^{\hat{z}_c} d\hat{z} (\hat{z}_c - \hat{z})^{-\frac{1}{2}} \rho_{\text{bs}} n_3 \quad (53) \end{aligned}$$

to within the order of the approximation entering (37) and (46).

The far-field version of the radial unit vector defined in (31) assumes the form

$$\lim_{r_P \rightarrow \infty} \hat{n} \Big|_{\phi=\phi_c, \hat{z}=\hat{z}_c} = \hat{r}^{-1} \hat{e}_{r_P} - (1 - \hat{r}^{-2})^{\frac{1}{2}} \hat{e}_{z_P} \quad (54)$$

on the cusp curve of the bifurcation surface [see (12b), (13) and (A27); and note that the position of the observer is here assumed to be such that the segment of the cusp curve lying within the source distribution is described by the expression with the plus sign in (12b), as in Fig. 6]. So, n_3 equals $\hat{n} \times \hat{e}_{\varphi_P}$ in the regime of validity of (53) [see (A45)]. Moreover, \hat{n} can be replaced by its far-field value

$$\hat{n} \simeq (\tau_P \hat{e}_{r_P} + z_P \hat{e}_{z_P}) / R_P, \quad R_P \rightarrow \infty, \quad (55)$$

if it is borne in mind that (53) holds true only for an observer the cusp curve of whose bifurcation surface intersects the source distribution.

Once n_3 in (53) is approximated by $\hat{n} \times \hat{e}_{\varphi_P}$ and the resulting \hat{z} -quadrature is expressed in terms of $\langle \rho_{bs} \rangle$ [see (38)], this equation reduces to

$$B \sim \hat{n} \times E, \quad (56)$$

where E is the electric field vector earlier found in (47). Equations (47) and (56) jointly describe a radiation field whose polarization vector lies along the direction of motion of the source, \hat{e}_{φ_P} .

Note that there has been no contribution toward the values of E and B from inside the bifurcation surface. These quantities have arisen in the above calculation solely from the jump discontinuities in the values of the Green's functions G_1^{out} , G_2^{out} and G_3^{out} across the coalescing sheets of the bifurcation surface. We would have obtained the same results had we simply excised the vanishingly small volume $\lim_{r_P \rightarrow \infty} V_{\text{in}}$ from the domains of integration in (29), (43) and (48).

Note also that the way in which the familiar relation (56) has emerged from the present analysis is altogether different from that in which it appears in conventional radiation theory. Essential though it is to the physical requirement that the directions of propagation of the waves and of their energy should be the same, (56) expresses a relationship between fields that are here given by non-spherically decaying surface integrals rather than by the conventional volume integrals that decay like r_P^{-1} .

V. A PHYSICAL DESCRIPTION OF THE EMISSION PROCESS

Expressions (47) and (56) for the electric and magnetic fields of the radiation that arises from a charge-current density with the components (23) and (39) imply the following Poynting vector:

$$\dot{S} \sim \frac{2^5}{3^2} \pi^{-1} c (c/\omega)^2 \hat{r}_P^{-1} \left[\int_{\hat{r}_<}^{\hat{r}_>} d\hat{r} \hat{r}^2 (\hat{r}^2 - 1)^{-\frac{1}{2}} (L_z \omega / c)^{\frac{1}{2}} \langle \rho_{bs} \rangle \right]^2 \hat{n}. \quad (57)$$

In contrast, the magnitude of the Poynting vector for the *coherent* cyclotron radiation that would be generated by a macroscopic lump of charge, if it moved subluminally with a centripetal acceleration $c\omega$, is of the order of $(\langle \rho \rangle L^3)^2 \omega^2 / (c R_P^2)$ according to the Larmor formula, where L^3 represents the volume of the source and $\langle \rho \rangle$ its average charge density. The intensity of the present emission is therefore greater than that of even a coherent conventional radiation by a factor of the order of $(L_z/L)(L\omega/c)^{-4}(R_P/L)$, a factor that ranges from 10^{16} to 10^{30} in the case of pulsars for instance.

The reason this ratio has so large a value in the far field ($R_P/L \gg 1$) is that the radiative characteristics of a volume-distributed source which moves faster than the waves it emits are radically different from those of a

corresponding source that moves more slowly than the waves it emits. There are source elements in the former case that approach the observer along the radiation direction with the wave speed at the retarded time. These lie on the intersection of the source distribution with what we have here called the bifurcation surface of the observer (see Figs. 5 and 6): a surface issuing from the position of the observer which has the same shape as the envelope of the wave fronts emanating from a source element (Figs. 1 and 3) but which spirals around the rotation axis in the opposite direction to this envelope and resides in the space of source points instead of the space of observation points.

The source elements inside the bifurcation surface of an observer make their contributions towards the observed field at three distinct instants of the retarded time. The values of two of these retarded times coincide for an interior source element that lies next to the bifurcation surface. This limiting value of the coincident retarded times represents the instant at which the component of the velocity of the source point in question equals the wave speed c in the direction of the observer. The third retarded time at which a source point adjacent to—just inside—the bifurcation surface makes a contribution is the same as the single retarded time at which its neighbouring source element just outside the bifurcation surface makes its contribution towards the observed field. (The source elements outside the bifurcation surface make their contributions at only a single instant of the retarded time).

At the instant marked by this third value of the retarded time, the two neighbouring source elements—just interior and just exterior to the bifurcation surface—have the same velocity, but a velocity whose component along the radiation direction is different from c . The velocities of these two neighbouring elements are, of course, equal at any time. However, at the time they approach the observer with the wave speed, the element inside the bifurcation surface makes a contribution towards the observed field while the one outside this surface does not: the observer is located just inside the envelope of the wave fronts that emanate from the interior source element but just outside the envelope of the wave fronts that emanate from the exterior one. Thus, the constructive interference of the waves that are emitted by the source element just outside the bifurcation surface takes place along a caustic which at no point propagates past the observer at the conical apex of the bifurcation surface in question.

On the other hand, the radiation effectiveness of a source element which approaches the observer with the wave speed at the retarded time is much greater than that of a neighbouring element the component of whose velocity along the radiation direction is subluminal or superluminal at this time. This is because the piling up of the emitted wave fronts along the line joining the

source and the observer makes the ratio of emission to reception time intervals for the contributions of the luminally moving source elements by many orders of magnitude greater than that for the contributions of any other elements. As a result, the radiation effectiveness of the various constituent elements of the source (i.e. the Green's function for the emission process) undergoes a discontinuity across the boundary set by the bifurcation surface of the observer.

The integral representing the superposition of the contributions of the various volume elements of the source to the potential thus entails a discontinuous integrand. When this volume integral is differentiated to obtain the field, the discontinuity in question gives rise to a boundary contribution in the form of a surface integral over its locus. This integral receives contributions from opposite faces of each sheet of the bifurcation surface which do not cancel one another. Moreover, the contributions arising from the exterior faces of the two sheets of the bifurcation surface do not have the same value even in the limit $R_P \rightarrow \infty$ where this surface is infinitely large and so its two sheets are—throughout a localized source that intersects the cusp—coalescent. Thus the resulting expression for the field in the radiation zone entails a surface integral such as that which would arise if the source were two-dimensional, i.e. if the source were concentrated into an infinitely thin sheet that coincided with the intersection of the coalescing sheets of the bifurcation surface with the source distribution.

For a two-dimensional source of this type—whether it be real or a virtual one whose field is described by a surface integral—the near zone (the Fresnel regime) of the radiation can extend to infinity, so that the amplitudes of the emitted waves are not necessarily subject to the spherical spreading that normally occurs in the far zone (the Fraunhofer regime). The Fresnel distance which marks the boundary between these two zones is given by $R_F \sim L_\perp^2/L_\parallel$, in which L_\perp and L_\parallel are the dimensions of the source perpendicular and parallel to the radiation direction. If the source is distributed over a surface and so has a dimension L_\parallel that is vanishingly small, therefore, the Fresnel distance R_F tends to infinity.

In the present case, the surface integral which arises from the discontinuity in the radiation effectiveness of the source elements across the bifurcation surface has an integrand that is in turn singular on the cusp curve of this surface. This has to do with the fact that the source elements on the cusp curve of the bifurcation surface approach the observer along the radiation direction not only with the wave speed but also with zero acceleration. The ratio of the emission to reception time intervals for the signals generated by these elements is by several orders of magnitude greater even than that for the elements on the bifurcation surface. When the contributions of these

elements are included in the surface integral in question, i.e. when the observation point is such that the cusp curve of the bifurcation surface intersects the source distribution (as shown in Fig. 6), the value of the resulting improper integral turns out to have the dependence $R_P^{-\frac{1}{2}}$, rather than R_P^{-1} , on the distance R_P of the observer from the source.

This non-spherically decaying component of the radiation is in addition to the conventional component that is concurrently generated by the remaining volume elements of the source. It is detectable only at those observation points the cusp curves of whose bifurcation surfaces intersect the source distribution. It appears, therefore, as a spiral-shaped wave packet with the same azimuthal width as the φ -extent of the source. For a source distribution whose superluminal portion extends from $\hat{r} = 1$ to $\hat{r} = \hat{r}_> > 1$, this wave packet is detectable—by an observer at infinity—within the angles $\frac{1}{2}\pi - \arccos \hat{r}_>^{-1} \leq \theta_P \leq \frac{1}{2}\pi + \arccos \hat{r}_>^{-1}$ from the rotation axis: projection (12b) of the cusp curve of the bifurcation surface onto the (τ, z) -plane reduces to $\cot \theta_P = (\hat{r}^2 - 1)^{\frac{1}{2}}$ in the limit $R_P \rightarrow \infty$, where $\theta_P \equiv \arctan(\tau_P/z_P)$ [also see (54)].

Because it comprises a collection of the spiralling cusps of the envelopes of the wave fronts that are emitted by various source elements, this wave packet has a cross section with the plane of rotation whose extent and shape match those of the source distribution. It is a diffraction-free propagating caustic that—when detected by a far-field observer—would appear as a pulse of duration $\Delta\varphi/\omega$, where $\Delta\varphi$ is the azimuthal extent of the source.

Note that the waves that interfere constructively to form each cusp, and hence the observed pulse, are different at different observation times: the constituent waves propagate in the radiation direction \hat{n} with the speed c , whereas the propagating caustic that is observed, i.e. the segment of the cusp curve that passes through the observation point at the observation time, propagates in the azimuthal direction \hat{e}_φ with the phase speed $r_P\omega$.

The fact that the intensity of the pulse decays more slowly than predicted by the inverse square law is not therefore incompatible with the conservation of energy, for it is not the same wave packet that is observed at different distances from the source: the wave packet in question is constantly dispersed and re-constructed out of other waves. The cusp curve of the envelope of the wavefronts emanating from an infinitely long-lived source is detectable in the radiation zone not because any segment of this curve can be identified with a caustic that has formed at the source and has subsequently travelled as an isolated wavepacket to the radiation zone, but because certain set of waves superpose coherently only at infinity.

Relative phases of the set of waves that are emitted during a limited time interval is such that these waves do not, in general, interfere construc-

tively to form a cusped envelope until they have propagated some distance away from the source. The period in which this set of waves has a cusped envelope and so is detectable as a periodic train of non-spherically decaying pulses, would of course have a limited duration if the source is short-lived.

Thus, pulses of focused waves may be generated by the present emission process which not only are stronger in the far field than any previously studied class of signals, but which can in addition be beamed at only a select set of observers for a limited interval of time.

VI. DESCRIPTION OF EXAMPLES OF THE APPARATUS

An apparatus can be designed for generating such pulses, in accordance with the above theory, which basically entails the simple components shown in Figs. 7(a) and 7(b).

Referring to the example of Fig. 7(a), a linear dielectric rod 1 of length l is provided with an array of electrodes 2, 3 arranged opposite one another along its length with n/l electrodes per unit length. In use, a voltage potential is applied across the dielectric rod 1 by the electrodes 2, 3, with each pair of electrodes 2, 3, in the array being activated in turn to generate a polarisation region with the fronts 5. By rapid application and removal of a potential voltage to electrodes 2, 3, this polarised region can be set in accelerated motion with a superluminal velocity. Creating a voltage across a pair of electrodes polarises the material in the rod between the electrodes. The electrodes can be controlled independently, so that the distribution pattern of polarisation of the rod as a function of length along the rod is controlled.

By varying the voltage across the electrode pairs as a function of time, this polarisation pattern is set in motion. For example, neighbouring electrode pairs can be turned on with a time interval of Δt between them, starting from one end of the rod. Thus, at a snapshot in time, part of the rod is polarised (that part lying between electrode pairs with a voltage across them) and part of it is not polarised (that part lying between electrode pairs without a voltage across them). These regions are separated by "polarisation fronts" which move with a speed of $l/(n\Delta t)$. With suitable choices of n and Δt the polarisation fronts can be made to move at any speed (including speeds faster than the speed of light *in vacuo*). The polarisation fronts can be accelerated through the speed of light by changing Δt with time.

High-frequency radiation may be generated by modulating the amplitude of the resulting polarisation current with a frequency Ω that exceeds a/c , where a is the acceleration of the source. The spectrum of the spherically decaying component of the radiation would then extend to frequencies that would be by a factor of the order of $(c\Omega/a)^2$ higher than Ω . The required

modulation may be achieved by varying the amplitudes of the voltages that are applied across various electrode pairs all in phase.

Figure 7(b) shows another example of the invention, the one analysed above. In this example, the dielectric rod is formed in the shape of a ring. Figure 7(b) is a plan view showing electrodes 2, and has electrodes 3 disposed below the rod 1. For a ring of radius r and a polarisation pattern that moves around the ring with an angular frequency ω , the velocity of the charged region is $r\omega$. In this example, $r\omega$ is greater than the speed of light c so that the moving polarisation pattern emits the radiation described with reference to Figures 1 to 6. An azimuthal or radial polarisation current may be produced by displacing the plates of each electrode pair relative to one another.

The voltages across neighbouring electrode pairs have the same time dependence (their period is $2\pi/\omega$) but, as in the rectilinear case, there is a time difference of Δt between them. The polarisation pattern must move coherently around the ring, i.e. must move rigidly with an unchanging shape; this would be the case if $n\Delta t = 2\pi N/\omega$, where n is the number of electrodes around the ring and N an integer. Within the confines of this condition, the time dependence of the voltage across each pair of electrodes can be chosen at will. The exact form of the adopted time dependence would allow, for example, the generation of harmonic content and structure in the source. As in the rectilinear case, modulation of the amplitude of this source at a frequency Ω would result in a radiation whose spectrum would contain frequencies of the order of $(\Omega/\omega)^2\Omega$.

The electrodes are driven by an array of similar oscillators, an array in which the phase difference between successive oscillators has a fixed value. There are several ways of implementing this:

- a single oscillator may be used to drive each electrode through progressively longer delay lines;

- each electrode pair may be driven by an individual oscillator in an array of phase-locked oscillators; or

- the electrode pairs may be connected to points around a circle of radius r which lies within—and is coplanar with—an annular waveguide, a waveguide whose normal modes include an electromagnetic wave train that propagates longitudinally around the circle with an angular frequency $\omega > c/r$.

For a dielectric rod in the shape of a ring of diameter 1 m, oscillators operating at a frequency of 100 MHz would generate a superluminally moving polarisation pattern. The required oscillator frequencies are easily obtainable using standard laboratory equipment, and any material with an appreciable polarizability at MHz frequencies would do for the medium. If the amplitude of the resulting polarisation current is in addition modulated at 1 GHz, then the device would radiate at ~ 100 GHz. The efficiency of this emission

process is expected to be as high as a few percent.

With oscillators operating at frequencies of 1 GHz (also available), the size of the device would be about 10 cm across; applications demanding portability are therefore viable.

VII. APPLICATIONS

A. Medical and biomedical applications

The present invention may be exploited to generate waves which do not form themselves into a focused pulse until they arrive at their intended destination and which subsequently remain in focus only for an adjustable interval of time, a property that allows for applications in various areas of medical practice and biomedical research.

Examples of its use in therapeutic medicine are: (i) the selective irradiation of deep tumours whilst sparing surrounding normal tissue, and (ii) the radiation pressure or thermocautery removal of thrombotic and embolic vascular lesions that may result from abnormalities in blood clotting without invasive surgery. Examples of its use in diagnostic medicine are absorption spectroscopy (focusing a broadband pulse within a tissue some frequencies of which would be absorbed) and three-dimensional tomography (mapping specifiable regions of interest within the body to high levels of resolution). In biomedical research, it provides a more powerful alternative to confocal scanning microscopy; with a single superluminal aerial being used as an X-ray source for imaging purposes.

An example of an apparatus required for generating the pulses in question is that shown in Fig. (7a). It consists of a linear dielectric rod, an array of electrode pairs positioned opposite to each other along the rod, and the means for applying a voltage to the electrodes sequentially at a rate sufficient to induce a polarization current whose distribution pattern moves along the rod with a constant acceleration at speeds exceeding the speed of light in *vacuo*.

The envelope of the wave fronts emanating from a volume element of the superluminally moving distribution pattern thus produced is shown in Fig. 8. It consists of a two-sheeted closed surface when the duration of the source includes the instant at which the source becomes superluminal. The two sheets of this envelope are tangent to one another and form a cusp along an expanding circle. If the source has a limited duration, the envelope in question is correspondingly limited [as in Fig. 9(d)] to only a truncated section of the surface shown in Fig. 8.

The snapshots in Fig. 9 trace the evolution in time of the relative posi-

tions of a particular set of wave fronts that are emitted during a short time interval. They include times at which the envelope has not yet developed a cusp [(a) and (b)], has a cusp [(c)-(e)], and has already lost its cusp (f).

A source with the life span $0 < t < T$ gives rise to a caustic, i.e. to a set of tangential wave fronts with a cusped envelope, only during the following finite interval of observation time:

$$M(M^2 - 1)l/c \leq t_P \leq M[M^2(1 + aT/u)^3 - 1]l/c, \quad (58)$$

where $M \equiv u/c$ and $l \equiv c^2/a$ with u , c , and a standing for the source speed at $t = 0$, the wave speed, and the constant acceleration of the source, respectively. For $aT/u \ll 1$, therefore, the duration of the caustic, $3M^2T$, is proportional to that of the source.

Moreover, a cusped envelope begins to form in the case of a short-lived source only after the waves have propagated a finite distance away from the source. The distance of the caustic from the position of the source at the retarded time is given by

$$\bar{R}_P = \beta_P^{\frac{1}{3}}(\beta_P^{\frac{2}{3}} - 1)l, \quad (59)$$

where $\beta_P \equiv (u + at_P)/c$ and t_P is the observation time. This distance can be long even when the duration of the source is short because there is no upper limit on the value of the length l ($\equiv c^2/a$) that enters (58) and (59): l tends to infinity for $a \rightarrow 0$ and is as large as 10^{18} cm when a equals the acceleration of gravity. Thus \bar{R}_P can be rendered arbitrarily large, by a suitable choice of the parameter l , without requiring either the duration of the source (T) or the retarded value ($\beta_P^{\frac{1}{3}}c$) of the speed of the source to be correspondingly large.

This means that, when either M or l is large, the waves emitted by a short-lived source do not focus to such an extent as to form a cusped envelope until they have travelled a long distance away from the source. The period during which they then do so can be controlled by adjusting the parameters M and T .

The collection of the cusp curves of the envelopes that are associated with various source elements constitutes a ring-shaped wave packet. This wave packet is intercepted only by those observers who are located, during its life time (58), on its trajectory

$$\xi = (\beta_P^{\frac{2}{3}} - 1)^{\frac{3}{2}}, \quad \zeta = \frac{1}{2}\beta_P^2 - \frac{3}{2}\beta_P^{\frac{2}{3}} + 1, \quad (60)$$

where ξ represents the distance (in units of l) of the observer from the rectilinear path of the source, say the z -axis, and ζ stands for the difference

between the Lagrangian coordinates $\bar{z} = z - ut - \frac{1}{2}at^2$ of the source point and $\bar{z}_P = z_P - ut_P - \frac{1}{2}at_P^2$ of the observation point.

It is possible to limit the spatial extent of the wave packet embodying the large-amplitude pulse by enclosing the path of the source within an opaque cylindrical surface which has a narrow slit parallel to its axis, a slit acting as an aperture that would only allow an arc of the ring-shaped wave packet to propagate to the far field. The volume occupied by the resulting wave packet could then be chosen at will by adjusting the width of the aperture and the longitudinal extent of the source distribution.

B. Compact sources of intense broadband radiation

In the near zone, the radiation that is generated by the invention can be arranged to have many features in common with synchrotron radiation. Most experiments presently carried out at large-scale synchrotron facilities could potentially be performed by means of a polarization synchrotron, i.e. the compact device described in Sec. VI. This device has applications, as a source of intense broadband radiation, in many scientific and industrial areas, e.g. in spectroscopy, in semiconductor lithography at very fine length scales, and in silicon chip manufacture involving UV techniques.

The spectrum of the radiation generated in a polarization synchrotron extends to frequencies that are by a factor of the order of $(c\Omega/a)^2$ higher than the characteristic frequency Ω of the fluctuations of the source itself (c and a are the speed of light and the acceleration of the source, respectively). For a polarizable medium consisting of a 1 m arc of a circular rod whose diameter is ~ 10 m [see Fig. (7b)], a superluminal source motion is achieved by an applied voltage that oscillates with the frequency ~ 10 MHz. If the amplitude of the resulting polarization current is in addition modulated at ~ 500 MHz, then the device would radiate at ~ 1 THz.

In the case of the source elements that approach the observer with the wave speed and zero acceleration, the interval of retarded time δt during which a set of waves are emitted is significantly longer than the interval of observation time δt_P during which the same set of waves are received.

For a rectilinearly moving superluminal source, the ratio $\delta t/\delta t_P$ is given by $2\frac{1}{2}(u^2/c^2 - 1)^{\frac{1}{2}}(a\delta t_P/c)^{-\frac{2}{3}}$, where u is the retarded speed of the source and a its constant acceleration. This ratio increases without bound as a approaches zero. Regardless of what the characteristic frequency of the temporal fluctuations of the source may be, therefore, it is possible to push the upper bound to the spectrum of the emitted radiation to arbitrarily high frequencies by making the acceleration a small. [Note that the emission process described here remains different from the Čerenkov process, in which a

exactly equals zero, even in the limit $a \rightarrow 0$.]

The relationship between δt and δt_P is $\delta t_P \simeq \frac{1}{6}\omega^2(\delta t)^3$ if the source moves circularly with the angular frequency ω . Thus the spectrum of the spherically decaying part of the radiation that is generated by accelerated superluminal sources extends to frequencies which are by a factor of the order of $(c\Omega/a)^2$ or $(\Omega/\omega)^2$ higher than the characteristic frequency Ω of the modulations of the source amplitude.

C. Long-range and high-bandwidth telecommunications

There are at present no known antennas in which the emitting electric current is both volume distributed and has the time dependence of a travelling wave with an accelerated superluminal motion. A travelling wave antenna of this type, designed on the basis of the principles underlying the present invention, generates focused pulses that not only are stronger in the far field than any previously studied class of signals, but can in addition be beamed at only a select set of observers for a limited interval of time: the constituent waves whose constructive interference gives rise to the propagating wave packet embodying a given pulse come into focus (develop a cusped envelope or a caustic) only long after they have emanated from the source and then only for a finite period (Fig. 9).

The intensity of the waves generated by this novel type of antenna decay much more slowly over distance than that of conventional radio or light signals. In the case of conventional sources, including lasers, if the transmitter (source) to receiver (destination) distance doubles, the power of the signal is reduced by a factor of four. With the present invention, the same doubling of distance only halves the available signal. Thus the power required to send a radio signal from the Earth to the Moon by the present transmitter would be 100 million times smaller than that which is needed in the case of a conventional antenna.

The emission mechanism in question can therefore be used to convey telephonic, visual and other electronic data over very long distances without significant attenuation. In the case of ground-to-satellite communications, the power required to beam a signal would be greatly reduced, implying that either far fewer satellites would be required for the same bandwidth or each satellite could handle a much wider range of signals for the same power output.

D. Hand-held communication devices

A combined effect of the slow decay rate and the beaming of the new

radiation is that a network of suitably constructed antennae could expand the useable spectrum of terrestrial electromagnetic broadcasts by a factor of a thousand or more, thus dispensing with the need for cable or optical fibre for high-bandwidth communications.

The evolution of the Internet, real-time television conferencing and related information-intense communication media means that there is a growing demand for cheap high-bandwidth aerials. Highly compact aerials for hand-held portable phones and/or television/Internet connections based on the present invention can handle, not only much longer transmitter-to-receiver distances than those currently available in cellular phone systems, but also much higher bandwidth.

Far fewer ground based aerial structures are required to obtain the same area coverage. Because there would be no cross-talk between any pairs of transmitter and receiver, the effective bandwidth of free space could be increased many thousand-fold, thus allowing, say, for video transmission between hand-held units.

APPENDIX A: ASYMPTOTIC EXPANSIONS OF THE GREEN'S FUNCTIONS

In this Appendix, we calculate the leading terms in the asymptotic expansions of the integrals (16), (34), (42) and (52) for small $\phi_+ - \phi_-$, i.e. for points close to the cusp curve (12) of the bifurcation surface (or of the envelope of the wavefronts). The method—originally due to Chester *et al.* (Proc. Camb. Phil. Soc., 54, 599, 1957)—which we use is a standard one that has been specifically developed for the evaluation of radiation integrals involving caustics (see Ludwig, Comm. Pure Appl. Maths, 19, 215, 1966). The integrals evaluated below all have a phase function $g(\varphi)$ whose extrema ($\varphi = \varphi_{\pm}$) coalesce at the caustic (12).

As long as the observation point does not coincide with the source point, the function $g(\varphi)$ is analytic and the following transformation of the integration variables in (16) is permissible:

$$g(\varphi) = \frac{1}{3}\nu^3 - c_1^2\nu + c_2, \quad (A1)$$

where ν is the new variable of integration and the coefficients

$$c_1 \equiv \left(\frac{3}{4}\right)^{\frac{1}{2}}(\phi_+ - \phi_-)^{\frac{1}{2}} \quad \text{and} \quad c_2 \equiv \frac{1}{2}(\phi_+ + \phi_-) \quad (A2)$$

are chosen such that the values of the two functions on opposite sides of (A1) coincide at their extrema. Thus an alternative exact expression for G_0 is

$$G_0 = \int_{-\infty}^{+\infty} d\nu f_0(\nu) \delta\left(\frac{1}{3}\nu^3 - c_1^2\nu + c_2 - \phi\right), \quad (A3)$$

in which

$$f_0(\nu) \equiv R^{-1}d\varphi/d\nu. \quad (A4)$$

Close to the cusp curve (12), at which c_1 vanishes and the extrema $\nu = \pm c_1$ of the above cubic function are coincident, $f_0(\nu)$ may be approximated by $p_0 + q_0\nu$, with

$$p_0 = \frac{1}{2}(f_0|_{\nu=c_1} + f_0|_{\nu=-c_1}), \quad (A5)$$

and

$$q_0 = \frac{1}{2}c_1^{-1}(f_0|_{\nu=c_1} - f_0|_{\nu=-c_1}). \quad (A6)$$

The resulting expression

$$G_0 \sim \int_{-\infty}^{+\infty} d\nu (p_0 + q_0\nu) \delta\left(\frac{1}{3}\nu^3 - c_1^2\nu + c_2 - \phi\right) \quad (A7)$$

will then constitute, according to the general theory, the leading term in the asymptotic expansion of G_0 for small c_1 .

To evaluate the integral in (A7), we need to know the roots of the cubic equation that follows from the vanishing of the argument of the Dirac delta function in this expression. Depending on whether the observation point is located inside or outside the bifurcation surface (the envelope), the roots of

$$\frac{1}{3}\nu^3 - c_1^2\nu + c_2 = 0 \quad (A8)$$

are given by

$$\nu = 2c_1 \cos\left(\frac{2}{3}n\pi + \frac{1}{3}\arccos\chi\right), \quad |\chi| < 1, \quad (A9a)$$

for $n = 0, 1$ and 2 , or by

$$\nu = 2c_1 \operatorname{sgn}(\chi) \cosh\left(\frac{1}{3}\operatorname{arccosh}|\chi|\right), \quad |\chi| > 1, \quad (A9b)$$

respectively, where

$$\chi \equiv [\phi - \frac{1}{2}(\phi_+ + \phi_-)] / [\frac{1}{2}(\phi_+ - \phi_-)] = \frac{3}{2}(\phi - c_2)/c_1^3. \quad (A10)$$

Note that χ equals $+1$ on the sheet $\phi = \phi_+$ of the bifurcation surface (the envelope) and -1 on $\phi = \phi_-$.

The integral in (A7), therefore, has the following value when the observation point lies inside the bifurcation surface (the envelope):

$$\int_{-\infty}^{+\infty} d\nu \delta\left(\frac{1}{3}\nu^3 - c_1^2\nu + c_2\right) = \sum_{n=0}^2 c_1^{-2} \left| 4 \cos^2\left(\frac{2}{3}n\pi + \frac{1}{3}\arccos\chi\right) - 1 \right|^{-1}, \quad |\chi| < 1. \quad (A11)$$

Using the trigonometric identity $4 \cos^2 \alpha - 1 = \sin 3\alpha / \sin \alpha$, we can write this as

$$\begin{aligned} \int_{-\infty}^{+\infty} d\nu \delta\left(\frac{1}{3}\nu^3 - c_1^2\nu + c_2\right) &= c_1^{-2} (1 - \chi^2)^{-\frac{1}{2}} \sum_{n=0}^2 \left| \sin\left(\frac{2}{3}n\pi + \frac{1}{3}\arccos\chi\right) \right| \\ &= 2c_1^{-2} (1 - \chi^2)^{-\frac{1}{2}} \cos\left(\frac{1}{3}\arcsin\chi\right), \quad |\chi| < 1, \end{aligned} \quad (A12)$$

in which we have evaluated the sum by adding the sine functions two at a time.

When the observation point lies outside the bifurcation surface (the envelope), the above integral receives a contribution only from the single value of ν given in (A9b) and we obtain

$$\int_{-\infty}^{+\infty} d\nu \delta\left(\frac{1}{3}\nu^3 - c_1^2\nu + c_2\right) = c_1^{-2} (\chi^2 - 1)^{-\frac{1}{2}} \sinh\left(\frac{1}{3}\operatorname{arccosh}|\chi|\right), \quad |\chi| > 1, \quad (A13)$$

where this time we have used the identity $4\cosh^2\alpha - 1 = \sinh 3\alpha / \sinh \alpha$.

The second part of the integral in (A7) can be evaluated in exactly the same way. It has the value

$$\begin{aligned} \int_{-\infty}^{+\infty} d\nu \nu \delta(\tfrac{1}{3}\nu^3 - c_1^2\nu + c_2) &= 2c_1^{-1}(1 - \chi^2)^{-\frac{1}{2}} \sum_{n=0}^2 |\sin(\tfrac{2}{3}n\pi + \tfrac{1}{3}\arccos\chi)| \\ &\quad \times \cos(\tfrac{2}{3}n\pi + \tfrac{1}{3}\arccos\chi) \\ &= -2c_1^{-1}(1 - \chi^2)^{-\frac{1}{2}} \sin(\tfrac{2}{3}\arcsin\chi), \quad |\chi| < 1, \quad (A14) \end{aligned}$$

when the observation point lies inside the bifurcation surface (the envelope), and the value

$$\int_{-\infty}^{+\infty} d\nu \nu \delta(\tfrac{1}{3}\nu^3 - c_1^2\nu + c_2) = c_1^{-1}(\chi^2 - 1)^{-\frac{1}{2}} \operatorname{sgn}(\chi) \sinh(\tfrac{2}{3}\operatorname{arccosh}|\chi|), \quad |\chi| > 1, \quad (A15)$$

when the observation point lies outside the bifurcation surface (the envelope).

Inserting (A12)–(A15) in (A7), and denoting the values of G_0 inside and outside the bifurcation surface (the envelope) by G_0^{in} and G_0^{out} , we obtain

$$G_0^{\text{in}} \sim 2c_1^{-2}(1 - \chi^2)^{-\frac{1}{2}} [p_0 \cos(\tfrac{1}{3}\arcsin\chi) - c_1 q_0 \sin(\tfrac{2}{3}\arcsin\chi)], \quad |\chi| < 1, \quad (A16)$$

and

$$G_0^{\text{out}} \sim c_1^{-2}(\chi^2 - 1)^{-\frac{1}{2}} [p_0 \sinh(\tfrac{1}{3}\operatorname{arccosh}|\chi|) + c_1 q_0 \operatorname{sgn}(\chi) \sinh(\tfrac{2}{3}\operatorname{arccosh}|\chi|)], \quad |\chi| > 1, \quad (A17)$$

for the leading terms in the asymptotic approximation to G_0 for small c_1 .

The function $f_0(\nu)$ in terms of which the coefficients p_0 and q_0 are defined is indeterminate at $\nu = c_1$ and $\nu = -c_1$: differentiation of (A1) yields $d\varphi/d\nu = (\nu^2 - c_1^2)/(\partial g/\partial\varphi)$ the zeros of whose denominator at $\varphi = \varphi_-$ and $\varphi = \varphi_+$ respectively coincide with those of its numerator at $\nu = +c_1$ and $\nu = -c_1$. This indeterminacy can be removed by means of l'Hopital's rule by noting that

$$\left. \frac{d\varphi}{d\nu} \right|_{\nu=\pm c_1} = \left. \frac{\nu^2 - c_1^2}{\partial g/\partial\varphi} \right|_{\nu=\pm c_1} = \left. \frac{2\nu}{(\partial^2 g/\partial\varphi^2)(d\varphi/d\nu)} \right|_{\nu=\pm c_1}, \quad (A18)$$

i.e. that

$$\left. \frac{d\varphi}{d\nu} \right|_{\nu=\pm c_1} = \left(\frac{\pm 2c_1}{\partial^2 g/\partial\varphi^2} \right)^{\frac{1}{2}} \bigg|_{\varphi=\varphi_{\mp}} = \frac{(2c_1 \hat{R}_{\mp})^{\frac{1}{2}}}{\Delta^{\frac{1}{4}}}, \quad (A19)$$

in which we have calculated $(\partial^2 g / \partial \varphi^2)_{\varphi=}$ from (7) and (8). The right-hand side of (A19) is, in turn, indeterminate on the cusp curve of the bifurcation surface (the envelope) where $c_1 = \Delta = 0$. Removing this indeterminacy by expanding the numerator in this expression in powers of $\Delta^{1/2}$, we find that $d\varphi/d\nu$ assumes the value $2^{1/2}$ at the cusp curve.

Hence, the coefficients p_0 and q_0 that appear in the expressions (A8) and (A9) for G_0 are explicitly given by

$$p_0 = (\omega/c)(\frac{1}{2}c_1)^{1/2}(\hat{R}_-^{-1/2} + \hat{R}_+^{-1/2})\Delta^{-1/2}, \quad (A20)$$

and

$$q_0 = (\omega/c)(2c_1)^{-1/2}(\hat{R}_-^{-1/2} - \hat{R}_+^{-1/2})\Delta^{-1/2} \quad (A21)$$

[see (A4)–(A6) and (A19)].

In the regime of validity of (A8) and (A9), where Δ is much smaller than $(\hat{r}_P^2 \hat{r}^2 - 1)^{1/2}$, the leading terms in the expressions for \hat{R}_\pm , c_1 , p_0 and q_0 are

$$\hat{R}_\pm = (\hat{r}_P^2 \hat{r}^2 - 1)^{1/2} \pm (\hat{r}_P^2 \hat{r}^2 - 1)^{-1/2} \Delta^{1/2} + O(\Delta), \quad (A22)$$

$$c_1 = 2^{-1/2} (\hat{r}_P^2 \hat{r}^2 - 1)^{-1/2} \Delta^{1/2} + O(\Delta), \quad (A23)$$

$$p_0 = 2^{1/2} (\omega/c) (\hat{r}_P^2 \hat{r}^2 - 1)^{-1/2} + O(\Delta^{1/2}), \quad (A24)$$

and

$$q_0 = 2^{-1/2} (\omega/c) (\hat{r}_P^2 \hat{r}^2 - 1)^{-1/2} + O(\Delta^{1/2}). \quad (A25)$$

These may be obtained by using (9) to express \hat{z} everywhere in (10), (11) and (A2) in terms of Δ and \hat{r} , and expanding the resulting expressions in powers of $\Delta^{1/2}$. The quantity Δ in turn has the following value at points $0 \leq \hat{z}_c - \hat{z} \ll (\hat{r}_P^2 - 1)^{1/2} (\hat{r}^2 - 1)^{1/2}$:

$$\Delta = 2(\hat{r}_P^2 - 1)^{1/2} (\hat{r}^2 - 1)^{1/2} (\hat{z}_c - \hat{z}) + O[(\hat{z}_c - \hat{z})^2], \quad (A26)$$

in which \hat{z}_c is given by the expression with the plus sign in (12b).

For an observation point in the far zone ($\hat{r}_P \gg 1$), the above expressions reduce to

$$\hat{R}_\pm \simeq \hat{r} \hat{r}_P, \quad c_1 \simeq 2^{1/2} (\hat{r} \hat{r}_P)^{-1/2} (1 - \hat{r}^{-2})^{1/2} (\hat{z}_c - \hat{z})^{1/2}, \quad (A27)$$

$$\Delta \simeq 2 \hat{r}_P (\hat{r}^2 - 1)^{1/2} (\hat{z}_c - \hat{z}), \quad (A28)$$

$$p_0 \simeq 2^{1/2} (\omega/c) (\hat{r}_P \hat{r})^{-1}, \quad q_0 \simeq 2^{-1/2} (\omega/c) (\hat{r}_P \hat{r})^{-2}, \quad (A29)$$

and

$$\chi \simeq 3(\frac{1}{2} \hat{r} \hat{r}_P)^{3/2} (1 - \hat{r}^{-2})^{-3/2} (\phi - \phi_c) / (\hat{z}_c - \hat{z})^{3/2}, \quad (A30)$$

in which $\bar{z}_c - \bar{z}$ has been assumed to be finite.

Evaluation of the other Green's functions, G_1 , G_2 and G_3 , entails calculations which have many steps in common with that of G_0 . Since the integrals in (34), (42) and (52) differ from that in (16) only in that their integrands respectively contain the extra factors \hat{n} , \hat{e}_φ and $\hat{n} \times \hat{e}_\varphi$, they can be rewritten as integrals of the form (A3) in which the functions

$$f_1(\nu) \equiv \hat{n}f_0, \quad f_2(\nu) \equiv \hat{e}_\varphi f_0 \quad \text{and} \quad f_3(\nu) \equiv \hat{n} \times \hat{e}_\varphi f_0 \quad (\text{A31})$$

replace the $f_0(\nu)$ given by (A4).

If p_0 and q_0 are correspondingly replaced, in accordance with (A5) and (A6), by

$$p_k = \frac{1}{2}(f_k|_{\nu=c_1} + f_k|_{\nu=-c_1}), \quad k = 1, 2, 3, \quad (\text{A32})$$

and

$$q_k = \frac{1}{2}c_1^{-1}(f_k|_{\nu=c_1} - f_k|_{\nu=-c_1}), \quad k = 1, 2, 3, \quad (\text{A33})$$

then every step of the analysis that led from (A7) to (A8) and (A9) would be equally applicable to the evaluation of G_k . It follows, therefore, that

$$G_k^{\text{in}} \sim 2c_1^{-2}(1 - \chi^2)^{-\frac{1}{2}}[p_k \cos(\frac{1}{3} \arcsin \chi) - c_1 q_k \sin(\frac{2}{3} \arcsin \chi)], \quad |\chi| < 1, \quad (\text{A34})$$

and

$$G_k^{\text{out}} \sim c_1^{-2}(\chi^2 - 1)^{-\frac{1}{2}}[p_k \sinh(\frac{1}{3} \operatorname{arccosh} |\chi|) + c_1 q_k \operatorname{sgn}(\chi) \sinh(\frac{2}{3} \operatorname{arccosh} |\chi|)], \quad |\chi| > 1, \quad (\text{A35})$$

constitute the uniform asymptotic approximations to the functions G_k inside and outside the bifurcation surface (the envelope) $|\chi| = 1$.

Explicit expressions for p_k and q_k as functions of (τ, z) may be found from (8), (A19), and (A31)–(A33) jointly. The result is

$$\begin{aligned} p_1 \\ q_1 = 2^{-\frac{1}{2}}(\omega/c)c_1^{\pm \frac{1}{2}}\Delta^{-\frac{1}{4}}\{[(\hat{r}_P - \hat{r}_P^{-1})(\hat{R}_-^{-\frac{3}{2}} \pm \hat{R}_+^{-\frac{3}{2}}) - \hat{r}_P^{-1}\Delta^{\frac{1}{2}}(\hat{R}_-^{-\frac{3}{2}} \\ \mp \hat{R}_+^{-\frac{3}{2}})]\hat{e}_{r_P} + \hat{r}_P^{-1}(\hat{R}_-^{-\frac{1}{2}} \pm \hat{R}_+^{-\frac{1}{2}})\hat{e}_{\varphi_P} + (\hat{z}_P - \hat{z})(\hat{R}_-^{-\frac{3}{2}} \pm \hat{R}_+^{-\frac{3}{2}})\hat{e}_{z_P}\}, \end{aligned} \quad (\text{A36})$$

$$\begin{aligned} p_2 \\ q_2 = 2^{-\frac{1}{2}}(\omega/c)(\hat{r}\hat{r}_P)^{-1}c_1^{\pm \frac{1}{2}}\Delta^{-\frac{1}{4}}\{(\hat{R}_-^{\frac{1}{2}} \pm \hat{R}_+^{\frac{1}{2}})\hat{e}_{r_P} \\ + [\hat{R}_-^{-\frac{1}{2}} \pm \hat{R}_+^{-\frac{1}{2}} + \Delta^{\frac{1}{2}}(\hat{R}_-^{-\frac{1}{2}} \mp \hat{R}_+^{-\frac{1}{2}})]\hat{e}_{\varphi_P}\}, \end{aligned} \quad (\text{A37})$$

and

$$\begin{aligned} p_3 &= 2^{-\frac{1}{2}}(\omega/c)(\hat{r}\hat{r}_P)^{-1}c_1 \pm \frac{1}{2}\Delta^{-\frac{1}{4}}\{-(\hat{z}_P - \hat{z})(\hat{R}_-^{-\frac{3}{2}} \pm \hat{R}_+^{-\frac{3}{2}} \\ q_3 &+ \Delta^{\frac{1}{2}}(\hat{R}_-^{-\frac{3}{2}} \mp \hat{R}_+^{-\frac{3}{2}})]\hat{e}_{r_P} + (\hat{z}_P - \hat{z})(\hat{R}_-^{-\frac{1}{2}} \pm \hat{R}_+^{-\frac{1}{2}})\hat{e}_{\varphi_P} \\ &+ \hat{r}_P[\Delta^{\frac{1}{2}}(\hat{R}_-^{-\frac{3}{2}} \mp \hat{R}_+^{-\frac{3}{2}}) - (\hat{r}^2 - 1)(\hat{R}_-^{-\frac{3}{2}} \pm \hat{R}_+^{-\frac{3}{2}})]\hat{e}_{z_P}\}, \quad (A38) \end{aligned}$$

where use has been made of the fact that $\hat{e}_\varphi = -\sin(\varphi - \varphi_P)\hat{e}_{r_P} + \cos(\varphi - \varphi_P)\hat{e}_{\varphi_P}$. Here, the expressions with the upper signs yield the p_k and those with the lower signs the q_k .

The asymptotic value of each G_k^{out} is indeterminate on the bifurcation surface (the envelope). If we expand the numerator of (A35) in powers of its denominator and cancel out the common factor $(\chi^2 - 1)^{\frac{1}{2}}$ prior to evaluating the ratio in this equation, we obtain

$$G_k^{\text{out}}|_{\phi=\phi_{\pm}} = G_k^{\text{out}}|_{\chi=\pm 1} \sim (p_k \pm 2c_1q_k)/(3c_1^2). \quad (A39)$$

This shows that $G_k^{\text{out}}|_{\phi=\phi_-}$ and $G_k^{\text{out}}|_{\phi=\phi_+}$ remain different even in the limit where the surfaces $\phi = \phi_-$ and $\phi = \phi_+$ coalesce. The coefficients q_k that specify the strengths of the discontinuities

$$G_k^{\text{out}}|_{\phi=\phi_+} - G_k^{\text{out}}|_{\phi=\phi_-} \sim \frac{4}{3}q_k/c_1 \quad (A40)$$

reduce to

$$q_1 \simeq \frac{3}{2^{\frac{1}{2}}}(\omega/c)(\hat{r}\hat{r}_P)^{-3}[(1 - \frac{2}{3}\hat{r}^2)\hat{r}_P\hat{e}_{r_P} + (\hat{z}_P - \hat{z})\hat{e}_{z_P}], \quad (A41)$$

$$q_2 \simeq 2^{\frac{1}{2}}(\omega/c)(\hat{r}\hat{r}_P)^{-1}\hat{e}_{\varphi_P}, \quad (A42)$$

and

$$q_3 \simeq -2^{\frac{1}{2}}(\omega/c)(\hat{r}\hat{r}_P)^{-2}[(\hat{z}_P - \hat{z})\hat{e}_{r_P} - \hat{r}_P\hat{e}_{z_P}] \quad (A43)$$

in the regime of validity of (A27) and (A28).

When $0 \leq \hat{z}_c - \hat{z} \ll (\hat{r}^2 - 1)^{\frac{1}{2}}\hat{r}_P$, the expressions (A41) and (A43) further reduce to

$$q_1 \simeq \frac{3}{2^{\frac{1}{2}}}(\omega/c)(\hat{r}\hat{r}_P)^{-2}n_1, \quad \text{and} \quad q_3 \simeq 2^{\frac{1}{2}}(\omega/c)(\hat{r}\hat{r}_P)^{-1}n_3, \quad (A44)$$

with

$$n_1 \equiv (\hat{r}^{-1} - \frac{2}{3}\hat{r})\hat{e}_{r_P} - (1 - \hat{r}^{-2})^{\frac{1}{2}}\hat{e}_{z_P} \quad \text{and} \quad n_3 \equiv (1 - \hat{r}^{-2})^{\frac{1}{2}}\hat{e}_{r_P} + \hat{r}^{-1}\hat{e}_{z_P}, \quad (A45)$$

for in this case (12b)—with the adopted plus sign—can be used to replace $\hat{z} - \hat{z}_P$ by $(\hat{r}^2 - 1)^{\frac{1}{2}}\hat{r}_P$.

CLAIMS

1. An apparatus for generating electromagnetic radiation comprising:

5 a polarizable or magnetizable medium; and means of generating, in a controlled manner, a polarization or magnetisation current whose distribution pattern has an accelerated motion with a superluminal speed, so that the apparatus generated both a non-spherically decaying
10 component and an intense spherically decaying component of electromagnetic radiation.

2. An apparatus according to claim 1, wherein the polarizable medium is a dielectric substrate.

15 3. An apparatus according to claim 2, wherein the means for generating the polarization current distribution is an array of electrode pairs positioned opposite to each other along the substrate and a voltage applied to the electrodes
20 sequentially at a rate sufficient to induce a polarization current whose distribution pattern moves along the substrate with a speed exceeding the speed of light in vacuo.

25 4. An apparatus according to any preceding claim, wherein the spectrum of the emitted electromagnetic radiation contains frequencies that are higher than the characteristic frequency of modulations of the emitting current.

30 5. An apparatus according to any preceding claim, where the polarizable or magnetizable has the shape of a circle or an arc of a circle.

35 6. An apparatus according to any of claims 1 to 4, where in the polarizable or magnetizable medium has a rectilinear shape.

7. An apparatus according to claim 6, wherein the distribution pattern of the current can be accelerated through the speed of light in such a way that the envelope of the wave fronts emitted by each volume element of this source possesses a cusp for a specific period of time.
8. A compact polarization synchrotron comprising an apparatus according to claims 4 and 5, arranged to generate intense, focused pulses of electromagnetic radiation with high frequencies in the near zone.
9. A device according to claims 7 and 8, arranged for spectroscopy.
10. A device according to claims 7 and 8, arranged for silicon chip manufacture and semiconductor lithography at very fine length scales.
11. A broad-band telecommunications antenna comprising an apparatus according to any preceding claim, for conveying telephonic, visual and other electronic data over very long distances without significant attenuation.
12. A broad-band telecommunications antenna comprising an apparatus according to claim 7, and means for controlling the apparatus such that a generated pulse of electromagnetic radiation is focused at a specific region of interest, distant from the antenna, for a specific period of time.
13. A network of antennae according to claims 11 and 12, arranged to expand the effective bandwidth of free space for terrestrial electromagnetic broadcasts and communications.

14. A highly compact aerial according to claims 11, 12 and 13 to be used for hand-held portable phones and/or television/Internet connections.

5 15. A device for medical diagnosis treatment comprising an apparatus according to claim 7, and means for controlling the apparatus such that a generated pulse of electromagnetic radiation is focused at a specific region of interest within the body for a specific period of time.

10

16. A device according to claim 15, arranged to irradiate deep tumours selectively whilst sparing surrounding normal tissue.

15

17. A device according to claim 15, arranged for radiation pressure or thermocautery removal of thrombotic and embolic vascular lesions without invasive surgery.

20

18. A device according to claim 15, arranged for three-dimensional tomography.

19. A device according to claim 15, arranged for absorption spectroscopy.

25

20. A device according to claim 15, arranged for confocal scanning microscopy.

30

1/9

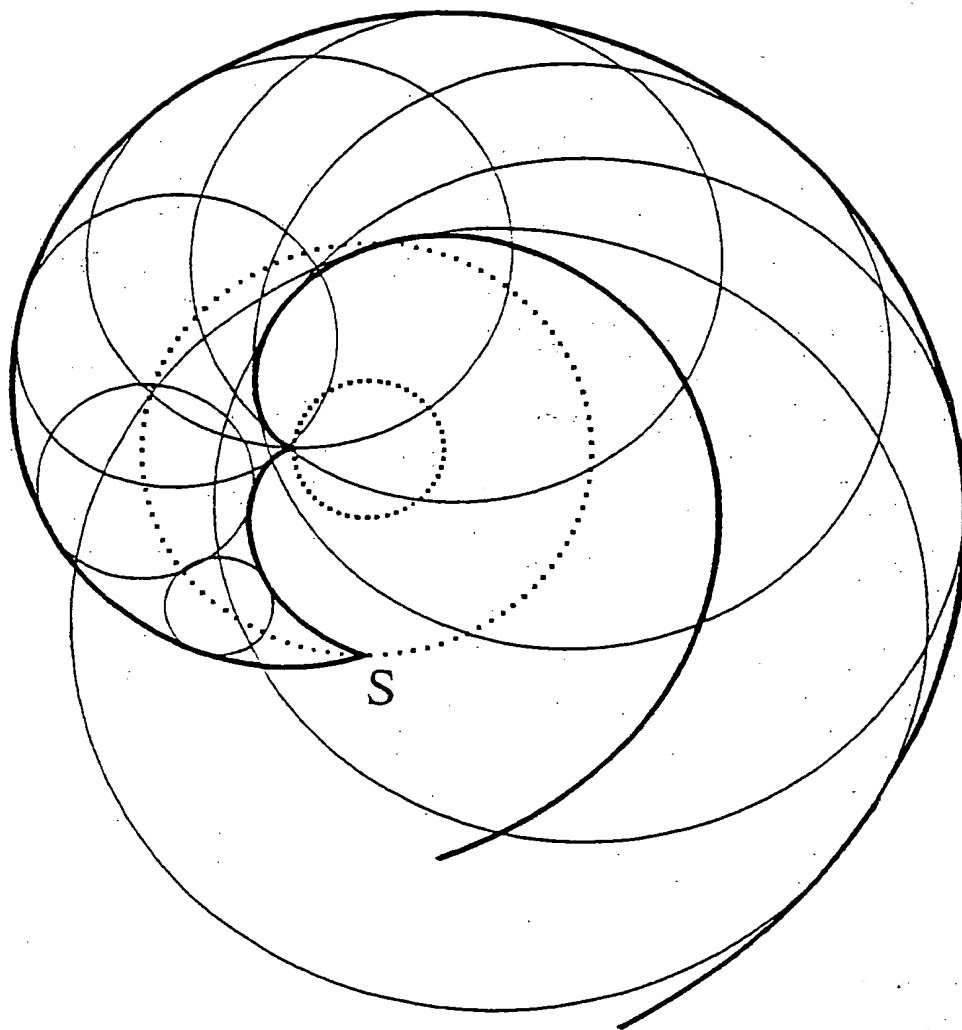


Figure 1

2/9

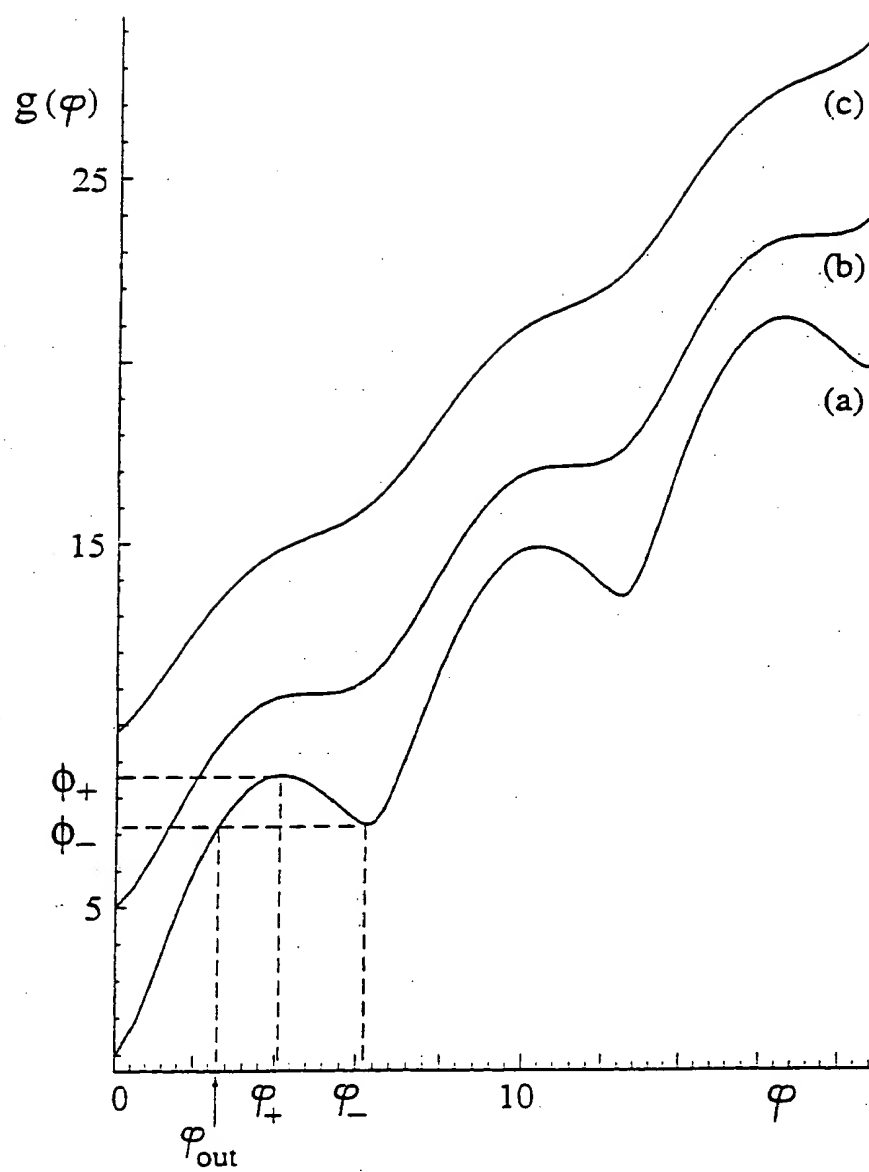


Figure 2

3/9

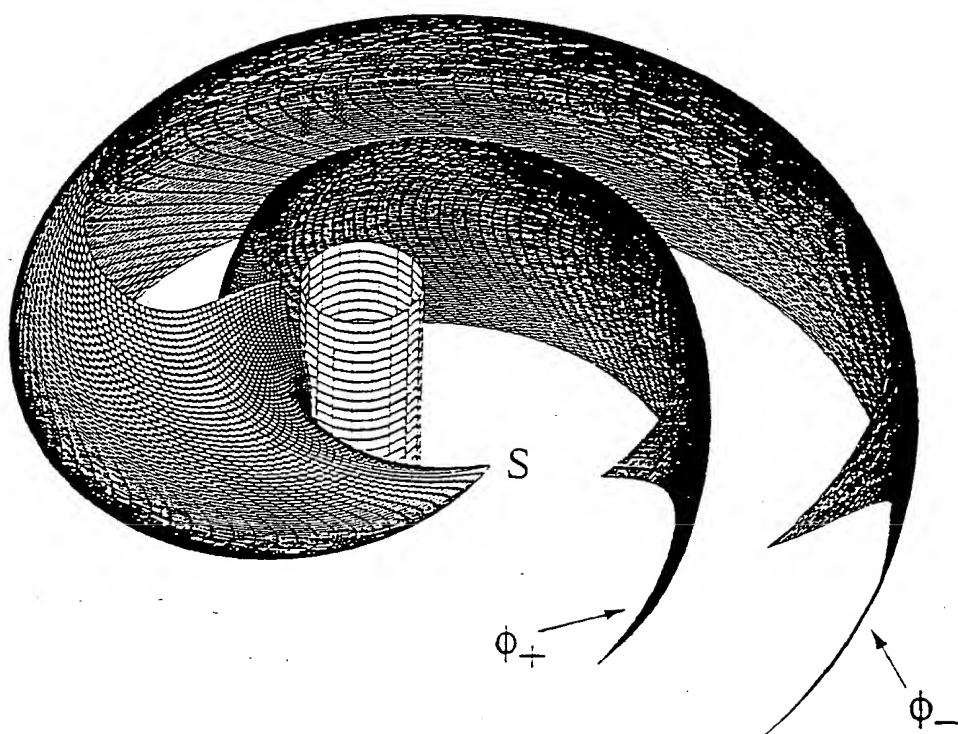


Figure 3

4/9

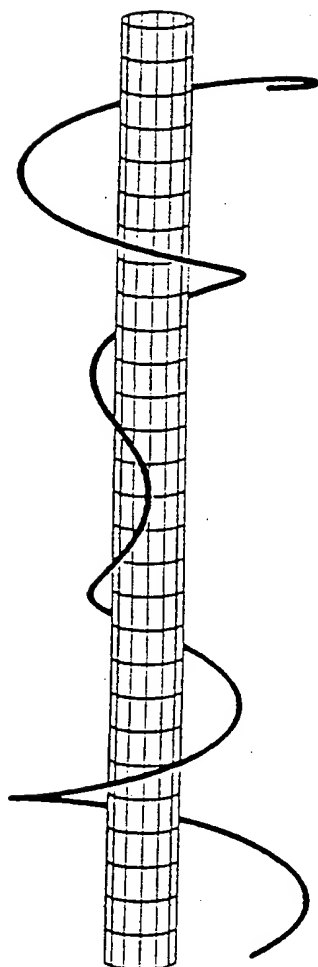


Figure 4

5/9

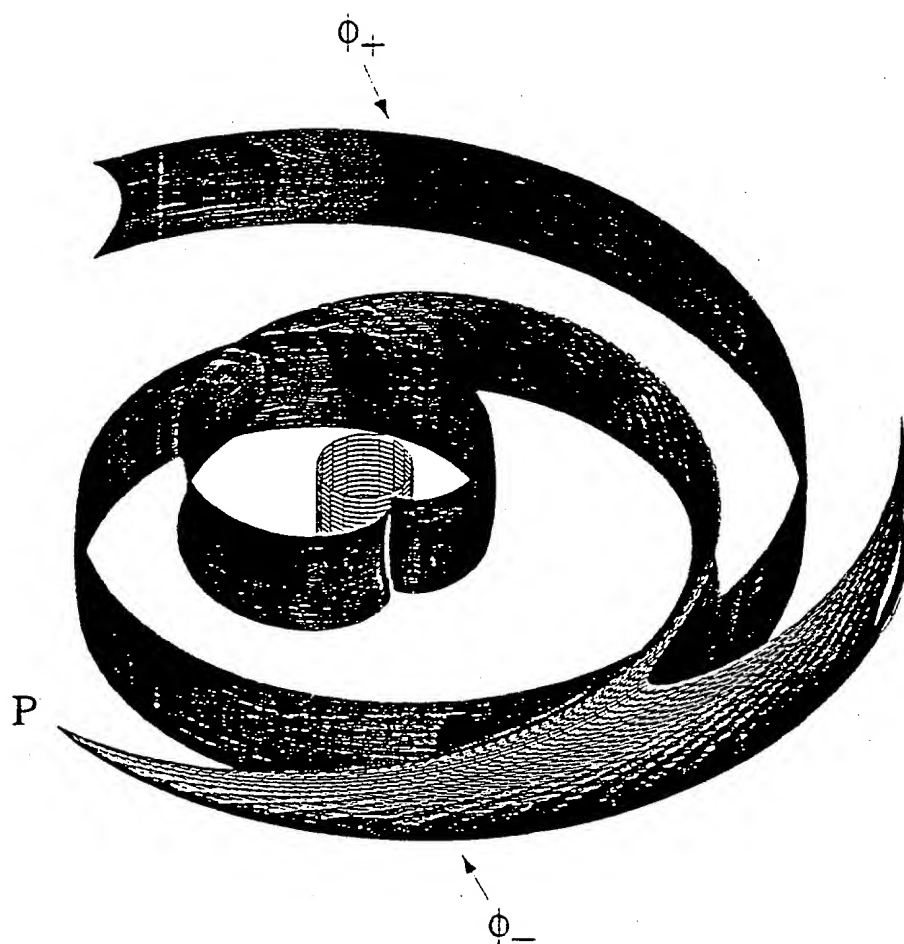


Figure 5

6/9

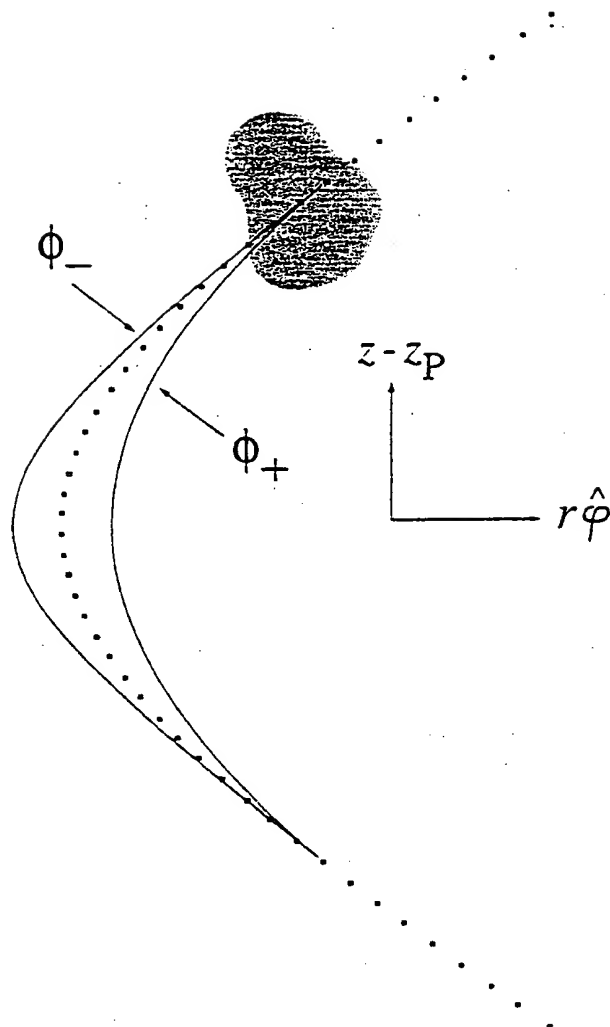
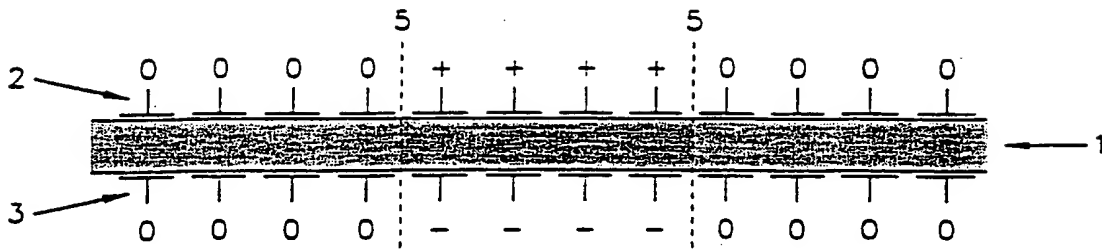


Figure 6

7/9

(a)

*(4 elements)*

(b)

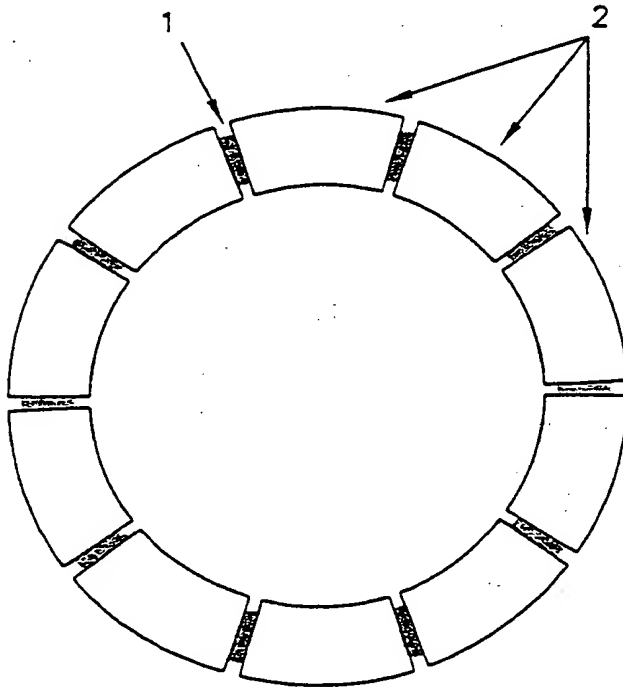


Figure 7

8/9

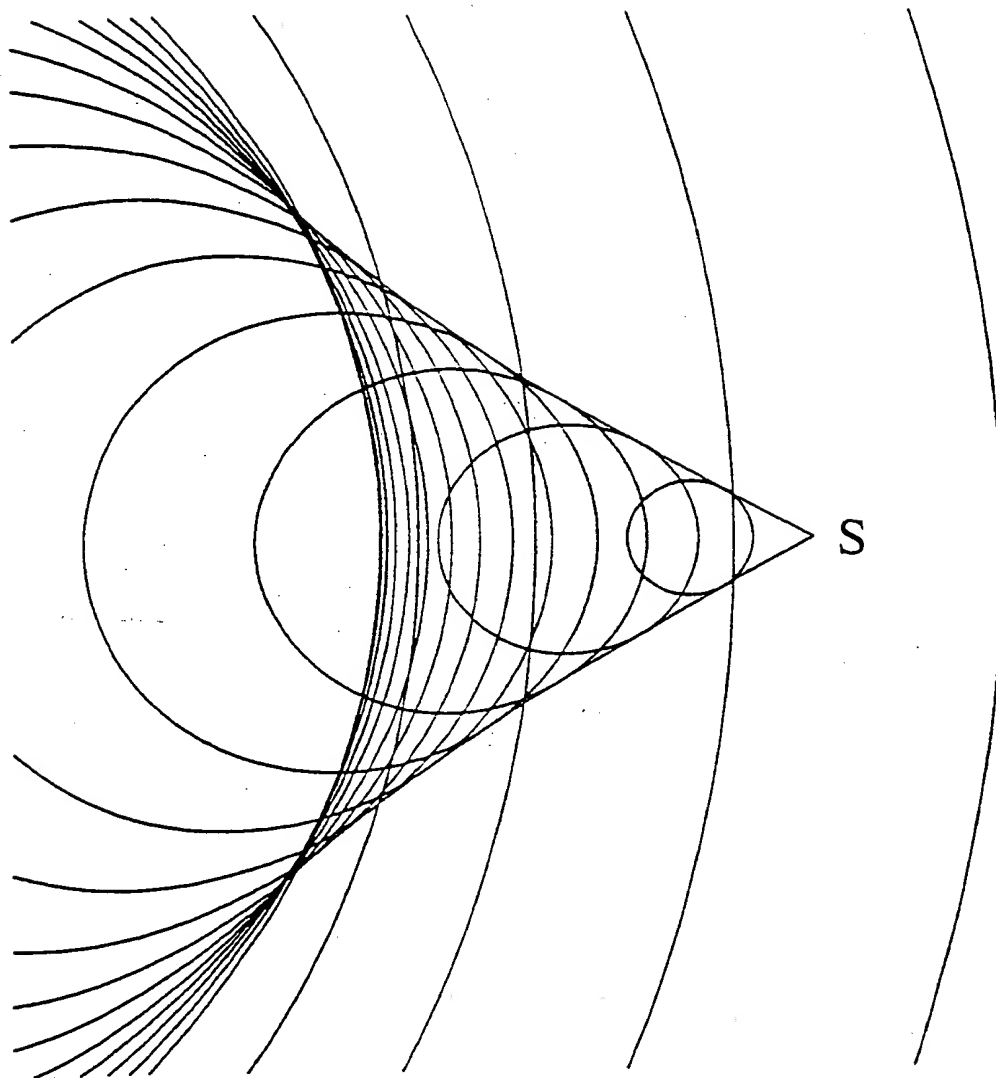


Figure 8

9/9

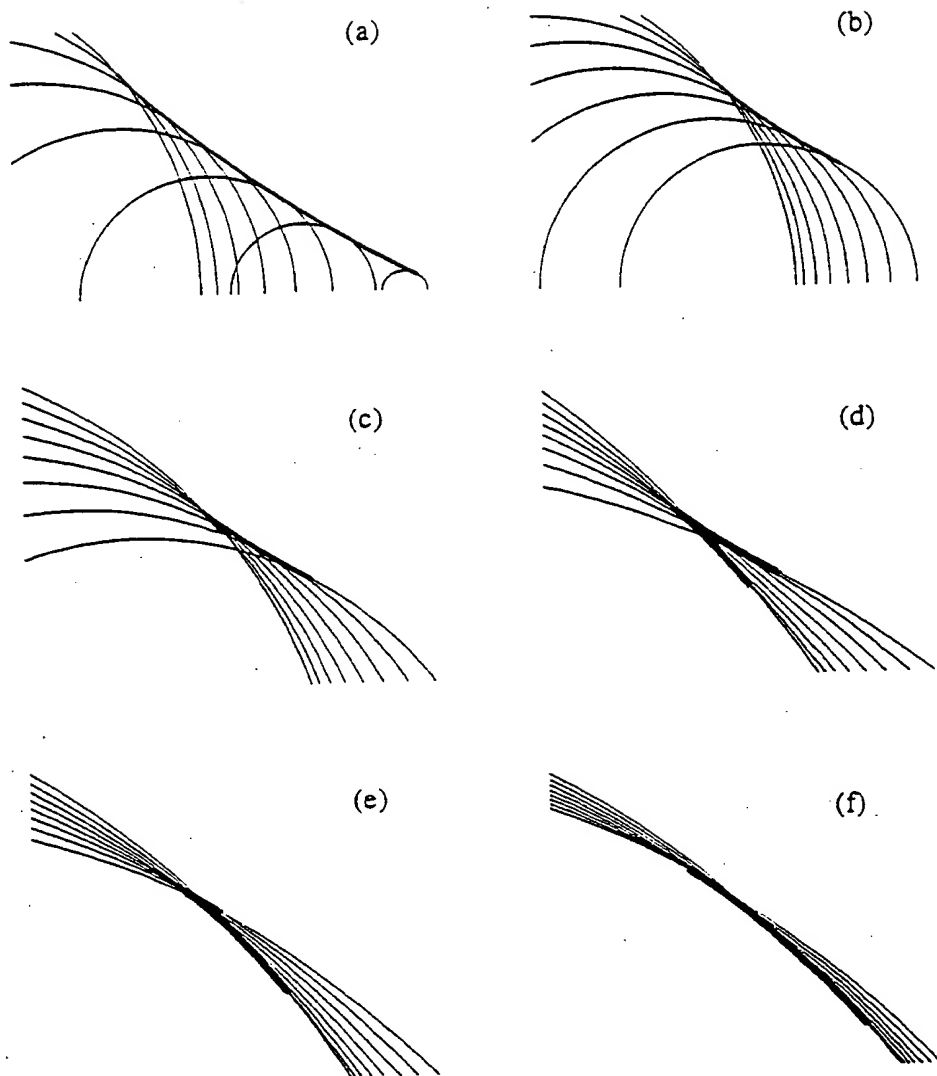


Figure 9

Office Action Summary

Application No.

09/786,507

Applicant(s)

ARDAVAN ET AL.

Examiner

Bernard E Souw

Art Unit

2881

-- The MAILING DATE of this communication appears on the cover sheet with the correspondence address --

Period for Reply

A SHORTENED STATUTORY PERIOD FOR REPLY IS SET TO EXPIRE 3 MONTH(S) FROM THE MAILING DATE OF THIS COMMUNICATION.

- Extensions of time may be available under the provisions of 37 CFR 1.136(a). In no event, however, may a reply be timely filed after SIX (6) MONTHS from the mailing date of this communication.
- If the period for reply specified above is less than thirty (30) days, a reply within the statutory minimum of thirty (30) days will be considered timely.
- If NO period for reply is specified above, the maximum statutory period will apply and will expire SIX (6) MONTHS from the mailing date of this communication.
- Failure to reply within the set or extended period for reply will, by statute, cause the application to become ABANDONED (35 U.S.C. § 133).
- Any reply received by the Office later than three months after the mailing date of this communication, even if timely filed, may reduce any earned patent term adjustment. See 37 CFR 1.704(b).

Status

- 1) ☒ Responsive to communication(s) filed on 06 March 2001.
- 2a) ☐ This action is FINAL. 2b) ☒ This action is non-final.
- 3) ☐ Since this application is in condition for allowance except for formal matters, prosecution as to the merits is closed in accordance with the practice under *Ex parte Quayle*, 1935 C.D. 11, 453 O.G. 213.

Disposition of Claims

- 4) ☒ Claim(s) 21-49 is/are pending in the application.
- 4a) Of the above claim(s) _____ is/are withdrawn from consideration.
- 5) ☐ Claim(s) _____ is/are allowed.
- 6) ☒ Claim(s) 21-49 is/are rejected.
- 7) ☒ Claim(s) 21-49 is/are objected to.
- 8) ☐ Claim(s) _____ are subject to restriction and/or election requirement.

Application Papers

- 9) ☒ The specification is objected to by the Examiner.
- 10) ☒ The drawing(s) filed on 06 March 2001 is/are: a) ☒ accepted or b) ☐ objected to by the Examiner.
- Applicant may not request that any objection to the drawing(s) be held in abeyance. See 37 CFR 1.85(a).
- 11) ☐ The proposed drawing correction filed on _____ is: a) ☐ approved b) ☐ disapproved by the Examiner.
- If approved, corrected drawings are required in reply to this Office action.
- 12) ☐ The oath or declaration is objected to by the Examiner.

Priority under 35 U.S.C. §§ 119 and 120

- 13) ☒ Acknowledgment is made of a claim for foreign priority under 35 U.S.C. § 119(a)-(d) or (f).
- a) ☒ All b) ☐ Some * c) ☐ None of:
1. ☒ Certified copies of the priority documents have been received.
2. ☐ Certified copies of the priority documents have been received in Application No. _____.
3. ☒ Copies of the certified copies of the priority documents have been received in this National Stage application from the International Bureau (PCT Rule 17.2(a)).
- * See the attached detailed Office action for a list of the certified copies not received.
- 14) ☐ Acknowledgment is made of a claim for domestic priority under 35 U.S.C. § 119(e) (to a provisional application).
- a) ☐ The translation of the foreign language provisional application has been received.
- 15) ☐ Acknowledgment is made of a claim for domestic priority under 35 U.S.C. §§ 120 and/or 121.

Attachment(s)

- 1) ☒ Notice of References Cited (PTO-892)
- 2) ☐ Notice of Draftsperson's Patent Drawing Review (PTO-948)
- 3) ☒ Information Disclosure Statement(s) (PTO-1449) Paper No(s) _____
- 4) ☐ Interview Summary (PTO-413) Paper No(s) _____
- 5) ☐ Notice of Informal Patent Application (PTO-152)
- 6) ☐ Other:

DETAILED ACTION

Priority

1. Receipt is acknowledged of papers submitted under 35 U.S.C. 119(a)-(d), (GB 9819504.3), which papers have been placed of record in the file.
2. Receipt is acknowledged of papers submitted under 35 U.S.C. 371 (PCT/GB99/02943) which papers have been placed of record in the file.

Preliminary Amendment

3. The Preliminary Amendment filed 03/06/2001, Paper #5/A, has been entered.

Specification

4. The disclosure is objected to because of the following informalities:
 - On page 1, paragraph 3, the wording "*intensities of normal emissions decay at a rate of R^2* ", does not conform with the general terminology accepted in the art, specifically regarding the words "*emission*", "*decay*", and "*rate*", these unusual words rendering the expression vague and not understandable to one of ordinary skill in the art. It is well known in the art that the intensity of a normal laser beam or laser "emission" (sic!) does **not** appreciably "decay" (sic!) over a significant distance R. Either Applicant's statement is incorrect, or Applicant meant a fully different thing than what he is trying to express with that highly unusual wording.

Even if Applicant is trying to mean something different, the statement regarding "decay at a rate of R^{-2} " is still not understandable, why it is worthwhile mentioning at all. It is generally known in the art that an **interference** normally **redistributes** the light intensity in such a way that it significantly deviates from a normal homogeneous distribution. Hence, the wording "decay at a rate of R^{-2} " has completely missed the point. A classic example is the previous example of a laser beam, which is basically a superposition of a whole bunch of mutually *interfering* electromagnetic *plane waves* having (slightly) differing propagation directions. Nobody would expressly appeal for attention that laser beams do not "decay at a rate of R^{-2} ".

5. The disclosure is **strongly** objected to because of the following inconsistencies already bordering to an incredibility of the invention:

- (a) On page 4, paragraph 2, line 2, the wording "**the superluminally rotating source** from the standpoint of geometrical optics" is in direct violation of a known law of nature, i.e., the Special Theory of Relativity, which prevents any material object from achieving luminal (let alone superluminal) speed in vacuum, since its mass would then become infinite, as generally understood in the art.
- (b) On page 6, paragraph 1, lines 1-2, the wording "so the speed of the source **exceeds** the wave speed", the wave speed being tacitly understood as being the light speed in vacuum, c , is again in direct violation of a known law of nature, i.e., the Special Theory of Relativity, by the same token as previously recited.

Art Unit: 2881

(c) On page 7, paragraph 3, line 1, the wording "*In the highly superluminal regime*" is again in direct violation of a known law of nature, by the same token as recited above.

(d) On page 27, paragraph 3, lines 7-8, the wording "*this polarized region can be set in accelerated motion with a superluminal velocity*" is again in direct violation of a known law of nature, by the same token as recited above.

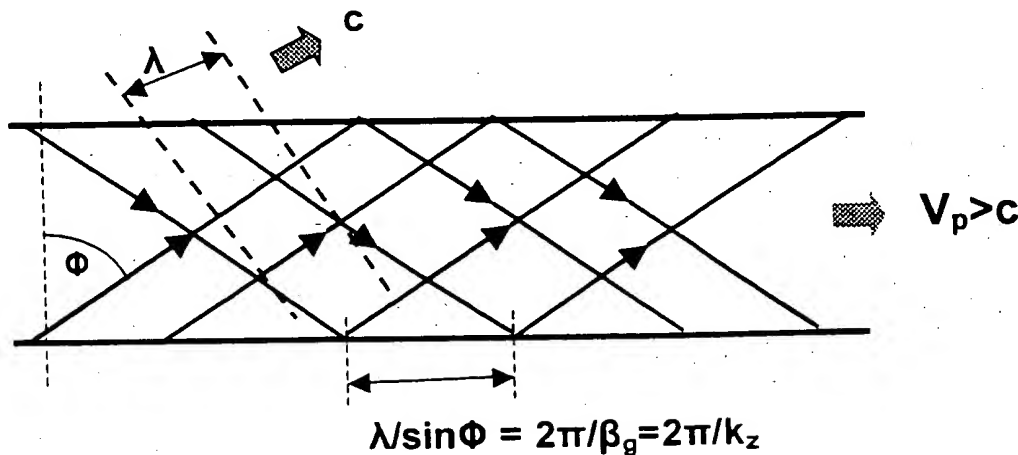
(e) Owing to the above objections, (a) to (d), and possibly still many others not yet discovered by the Examiner, the credibility of the invention is very strongly put in question, for its obvious violation against a known law of nature. Although in a few other occasions Applicant seems to vaguely avoid such violation, as reflected on page 2, paragraph 2, line 1, by reciting "*The speed of the moving **distribution pattern** may be superluminal*", and again on page 3, paragraph 3, lines 4-5, by reciting "*whose distribution **patterns** propagate with a phase speed exceeding the speed of light in vacuo*" << which are here not objected because a pattern is not a material object (in this case the material object may not be moving at all), and hence, may well achieve, or even exceed, the speed of light in vacuo, c >>, these statements have been effectively overridden by more frequently recited contradicting statements claiming on superluminal velocities of material objects throughout the entire disclosure. Such a violation of natural law leads to a §101 rejections based on incredibility of the invention and/or its inoperativeness, as well as to a §112/¶.1 claim rejections based on enablement and §112/¶.2 claim rejections based on indefiniteness (see Claim Rejections below).

Corrections are required. Applicant is advised, not to introduce New Matter in obviating this objection.

Art Unit: 2881

(f) Applicant is advised to eliminate the misleading word "*superluminal*" entirely from the disclosure. Applicant's terminology "*superluminal*" is misleading, because in fact there is **no superluminal speed** at all. "Superluminally" moving patterns, e.g., phase patterns, or field/voltage patterns, have been known in the art for almost the age of electromagnetic theory itself, as it routinely occurs in electromagnetic waveguides. This is a fact that can be found in almost every textbook on electromagnetic waveguides, e.g., "Introduction to Microwave Theory" by Atwater (1962), as specifically recited on page 82, lines 8-10, in reference to Fig. 3.2 on page 59 and Eq. 3.137 on page 81 (see attached PTO-892). The e.m. wave in a waveguide can be considered as a superposition of two plane waves reflected to and fro between the waveguide walls at an angle Φ (see Fig.1 below).

Fig. 1: Wavefronts and Phase Velocity in a Waveguide



The phase velocity V_p in the waveguide propagation direction z is defined by Atwater's Eq. 3.136. Although the phase velocity perpendicular of the wavefront remains equal to c , the phase velocity in the z direction is $V_p = c/\sin\Phi$, which is always larger than c for

Art Unit: 2881

$\Phi > 0$. At the waveguide cut-off ($\beta_g = 0$) the phase velocity approaches infinity (see Atwater's Fig. 3.2).

In case of Applicant's invention, the wave propagation into free space does not differ much from the waveguide situation above, here easily replicated by substituting one of the waveguide walls by an antenna array while eliminating the other, thus removing the reflected waves. Although the phase or voltage pattern along the antenna array (waveguide wall) is still moving in the z direction at a "*superluminal*" velocity, $V_P > c$, the wave velocity propagating into free space remains equal to c . In other words, there is **no real** superluminal velocity involved. Interference between adjacent array elements causes the wavefront of the emitted wave propagate at an angle Φ , as recited by Hopwood et al. (USPAT # 4,749,995) in Col.2/ll.40-47 in reference to Fig.1, and by O'Donnell et al. (USPAT 4,809,184) in Col.4/ll.30-35 and Col.5/ll.20-30 in reference to Fig.1.

Based on the discussion above, claim limitations reciting any ***distribution pattern*** moving at "*superluminal*" velocities, such as recited in claims 21, 23 and 27, are inappropriate. Although not principally incorrect, such limitation is misleading, for reciting something that is completely irrelevant to the subject matter of the invention, and furthermore, has no significance in the real world. Although the phase velocity in a waveguide is always greater than c , it is the group velocity that is relevant to the real world, e.g., as communication signal carrier. This group velocity is always less than c .

Applicant's invention has *much less* to do with current distribution pattern moving at superluminal velocities rather than with beam steering and beam focusing of a

phased array antenna. The latter has been well known since many decades in a diverse area such as radar technology (Hogwood et al., 1988), directed energy weapons (Ensley 1984, USPAT 4,456,912) and medical diagnostics and therapy (Cori, 1990, USPAT 4,974,211).

In contradiction to Applicant's claim, there is evidently no superluminal wave propagation or any other anomaly generated by any of the methods using any of the antenna configurations disclosed as Applicant's invention. The observed result is nothing else than a normal (luminal) beam radiated at a variable angle Φ . In view of the overwhelming evidences brought up in this Office Action (see PTO-892), the burden of proof returns back to the Applicant's side in case Applicant insists the invention is capable of generating superluminal or any other unique form of light propagation.

(g) The lengthy specification has not been checked to the extent necessary to determine the presence of all possible errors of the same type as recited above from (a) to (d). Applicant's cooperation is requested in correcting any errors of which applicant may become aware in the specification.

Claim Rejections - 35 USC § 101

35 U.S.C. 101 reads as follows:

Whoever invents or discovers any new and useful process, machine, manufacture, or composition of matter, or any new and useful improvement thereof, may obtain a patent therefor, subject to the conditions and requirements of this title.

6. Claims 21, 23 and 27 are rejected under 35 U.S.C. 101 because the claimed invention is not supported by either a specific asserted utility or a well-established utility.

Art Unit: 2881

Claims 21, 23 and 27 recite limitations of a superluminal velocity, or a velocity exceeding the velocity of light in vacuo. Since the disclosure recite specific statements that indicate a violation of physical law(s), claims 21, 23 and 27 are deemed incredible when interpreted in light of the specification, and hence, are not supported by a well established utility. Even if the claims are interpreted in such a way so as to avoid any violation of natural laws, the recitations of "*polarization current **distribution** that moves with superluminal velocity*" in claims 21, 23 and 27, and also "*the envelope of the wavefronts ... possesses a **cusp***" specifically recited in claim 27, have no significance in the real world, as already pointed out in the previous objection to the specification with the exemplary discussion on phase and group velocities in a waveguide. Hence, the claims lack any specific asserted utility.

Use Claim

7. Claims 30-49 are rejected under 35 U.S.C. 101 because the claimed recitation of a use, without setting forth any steps involved in the process, results in an improper definition of a process, i.e., results in a claim which is not a proper process claim under 35 U.S.C. 101. See for example *Ex parte Dunki*, 153 USPQ 678 (Bd.App. 1967) and *Clinical Products, Ltd. v. Brenner*, 255 F. Supp. 131, 149 USPQ 475 (D.D.C. 1966).

Consequently, claims 30-49 are excluded from all first office actions on the merits and final rejections.

Claim Rejections - 35 USC § 112 / 1st paragraph

The following is a quotation of the first paragraph of 35 U.S.C. 112:

The specification shall contain a written description of the invention, and of the manner and process of making and using it, in such full, clear, concise, and exact terms as to enable any person skilled in the art to which it pertains, or with which it is most nearly connected, to make and use the same and shall set forth the best mode contemplated by the inventor of carrying out his invention.

8. Claims 21, 23 and 27 are also rejected under 35 U.S.C. 112, first paragraph. Specifically, since the claimed invention is not supported by either a specific asserted utility or a well established utility for the reasons set forth above, one skilled in the art clearly would not know how to use the claimed invention.

Claim Rejections - 35 USC § 112/ 2nd paragraph

The following is a quotation of the second paragraph of 35 U.S.C. 112:

The specification shall conclude with one or more claims particularly pointing out and distinctly claiming the subject matter which the applicant regards as his invention.

9. Claims 21, 23 and 27 are also rejected under 35 U.S.C. 112, second paragraph, as being indefinite for failing to particularly point out and distinctly claim the subject matter which applicant regards as the invention.

The independent claim 21, from which claims 23 and 27 depend, fails to identify the particular electrode configuration being used to generate polarization current: It is not at all clear, whether it is a configuration shown in any one of Fig.1 to Fig.6, or any one shown in Fig.7? Specific electrode configuration is only recited in claim 25 as being the configuration of Fig.7b, and in claim 26 as being the configuration shown in Fig.7a. In regards of this ambiguity, the specific means to apply the polarizing voltage to, or polarization current into, the polarizable medium critical or essential to the practice of

Art Unit: 2881

the invention but not included in the claim(s), is not enabled by the disclosure. See *In re Mayhew*, 527 F.2d 1229, 188 USPQ 356 (CCPA 1976).

In order to proceed with this examination, a linear electrode configuration as depicted in Fig.7a is assumed by the examiner. However, for claim 25 the configuration of Fig.7b will be assumed, despite its inconsistency with the dependent claim 21. It is thus obvious that all the claims here involved have to be reformulated.

Use Claims

10. Claims 30-49 provide for the use of the invention for various applications, ranging from spectroscopy over semiconductor manufacturing process to medical applications, but, since the claims do not set forth any steps involved in the respective method/process, it is unclear what method/process applicant is intending to encompass. A claim is indefinite where it merely recites a use without any active, positive steps delimiting how this use is actually practiced.

Consequently, claims 30-49 are excluded from all first office actions on the merits and final rejections.

Claim Rejections - 35 USC § 102

The following is a quotation of the appropriate paragraphs of 35 U.S.C. 102 that form the basis for the rejections under this section made in this Office action:

A person shall be entitled to a patent unless –

(b) the invention was patented or described in a printed publication in this or a foreign country or in public use or on sale in this country, more than one year prior to the date of application for patent in the United States.

Art Unit: 2881

11. Insofar the Examiner can ascertain beyond the above rejection under the first and second paragraphs of 35 U.S.C. 112, claims 21-22 are rejected under 35 U.S.C. 102(b) as being anticipated by Bridges (USPAT 5,704,355).

Bridges discloses an apparatus for generating electromagnetic radiation as expressly recited in Col.2/ll.20-22, comprising a polarizable medium 410A to 410D depicted in Fig.14, as recited in Col.16/ll.1-14; and means of generating a polarization current whose distribution pattern moves with a superluminal speed, as recited in Col.16/ll.16-34, whereby the superluminal speed is inherently recited in Col.16/ll.29-34 in reference to Fig.14, i.e., in case the device is used for wave propagation in free space, so the medium 418 is air or vacuum and V is equal to c in the formulae recited in Col.16/ll.31-33.

Although Bridges's invention is more directed to medical treatment, in which the medium 418 is human tissue, and hence, $v < c$, Bridges expressly recites in Col.2/ll.16-36, even more clearly in Col.2/ll.55-67 & Col.3/ll.5-15, that the invention is derived from and hence, inherently also applicable to open air or vacuum environment. Thus, an equivalent e.m. system operating in air or vacuum is inherent in O'Donell's, including appropriate changes such as air or vacuum for medium 418, and that V is equal to c .

► Specifically regarding the limitation of the distribution pattern having an **accelerated** motion with a superluminal speed, as recited in claim 21, such motion is known to focus the radiated beam, as inherently understood from Col.16/ll.29-34.

Art Unit: 2881

► Specifically regarding the limitation of the radiated e.m. wave consisting of both non-spherically decaying component and a spherically decaying component, as recited in claim 21, an interfering wavefronts can always be inherently considered as a superposition of non-spherically decaying component having an inhomogeneous intensity distribution $\sim R^x$ with $x < 2$ (such as a laser as an extreme representative), and a spherically decaying (non-interfering) component having a homogeneous intensity distribution $\sim R^{-2}$.

► Regarding claim 22, Bridges's polarizable medium, i.e., the most important part of the antenna 410A-410D in Fig.14, is a dielectric substrate, as expressly recited in Col.22/ll.33-34.

Claim Rejections - 35 USC § 103

12. The following is a quotation of 35 U.S.C. 103(a) which forms the basis for all obviousness rejections set forth in this Office action:

(a) A patent may not be obtained though the invention is not identically disclosed or described as set forth in section 102 of this title, if the differences between the subject matter sought to be patented and the prior art are such that the subject matter as a whole would have been obvious at the time the invention was made to a person having ordinary skill in the art to which said subject matter pertains. Patentability shall not be negated by the manner in which the invention was made.

Insofar the Examiner can ascertain beyond the above rejection under the first and second paragraph of 35 U.S.C. 112, claims 23-24 and 26-28 are rejected under 35 U.S.C. 103(a) as being unpatentable over Bridges in view of Miller (USPAT 4,131,896) or Nunnally (IEEE Transactions on Electron Devices Vol.17/No.12, 1990, pp.2439-2445) in further view of Zucker et al. (USPAT 5,109,203), hereafter referred to as Zucker-203.

13. Bridges shows all the limitations of claim 23, as applied previously to the parent claim 22, except the recitation of electrode pairs positioned opposite to each other as a means to induce the polarization current of claims 21 and 22.

Miller discloses an apparatus for generating electromagnetic radiation equipped with electrode pairs, 36 & 20, as recited in Col.5/ll.13-19, positioned opposite to each other as a means to induce the polarization current in the radiating elements 26, as recited in Col.4/ll.66-68 & Col.5/ll.1-66 in reference to Fig.6. While Miller's invention is primarily aimed at compensating for impedance variations over the scan angle, as recited in the Title and Abstract, it would have been obvious to one of ordinary skill in the art by the time the invention was made to feed Miller's antenna array with conventional phase controlled electromagnetic signal, as readily taught by Bridges, i.e., by using time delays applied to phase control devices 408, as recited in Col.16/ll.10-41.

Note, time delay and phase control are representing the same method of beam steering in phased arrays, since a time delay automatically results in a phase shift of the signal wave. The terminology "*time delay*" is usually used in case of pulsed beams, whereas "*phase control*" or "*phase shift*" is more appropriate for continuous wave (cw) electromagnetic beams.

Miller's modification applies in case the means of applying voltage or current, hereafter simply denoted as "*applicator*", is designed as an antenna array that allows wave transmission in the angular range of $\Phi < 90^\circ$ to $\Phi = 0^\circ$, but effectively blocks or excludes the $\Phi = 90^\circ$ direction (please refer to Fig.1 of this Office Action for a definition of

Art Unit: 2881

Φ). In this case the polarization current distribution pattern applied to the array moves with $V_p > c$ (corresponding to $\Phi < 90^\circ$) to infinity (corresponding to $\Phi = 0^\circ$).

It would have been obvious to one of ordinary skill in the art by the time the invention was made to modify Bridges's array of horn antenna elements by Miller's capacitor-like dipole antennas, in order to have the capability of scanning the angular direction perpendicular to the array, and to have an antenna array with uniform impedance across the scan range, as taught by Miller.

14. Alternatively, claim 23 is rejected under 35 U.S.C. 103(a) as being unpatentable over Bridges in view of Nunnally and further in view of Zucker-203. This alternative rejection is applicable in case the "*applicator*" is designed as an antenna array that blocks wave transmission in the angular range of $\Phi < 90^\circ$ to $\Phi = 0^\circ$, i.e., as linear capacitor array depicted in Fig. 7a of Applicant's disclosure. As generally known in the art, the generated electromagnetic wave propagates along the transmission line ($\Phi = 90^\circ$) at a velocity given by the wave velocity of the transmission line formed by the sequentially connected capacitors.

Nunnally discloses an apparatus for generating electromagnetic radiation equipped with electrode pairs positioned opposite to each other as a means to induce polarization current, as shown in Fig.8 and recited on page 2444, section A. "Frozen-Wave Generator", paragraph 1 & 2.

It would have been obvious to one of ordinary skill in the art by the time the invention was made to modify Bridges's array of horn antenna elements by Nunnally's

Art Unit: 2881

linear array of capacitors forming a transmission line, in order to transmit the e.m. signal along the capacitor array, since the performance characteristics of such a transmission line is well known in the art, so as to render the design straightforward and the effort requirement minimum.

While Nunnally's frozen-wave generator transmits a pulsed e.m. wave of a particular square-wave form that has been previously "frozen" in the capacitor array, in case of a continuous wave it would have been further obvious to one of ordinary skill in the art by the time the invention was made to further modify Bridges's device that has been previously modified by Nunnally's, now also by Zucker-203 as depicted in Fig.4A and Fig.3 & 4, with Zucker-203's time-trigger diodes 28, 30, 32 in Fig.1C replaced by Nunnally's photoconductive triggers shown in Fig.8, while using Zucker-203's horn antenna 26 shown in Fig. 3 & 4 to transmit the e.m. wave in a quasi-continuous manner.

Thus, instead of releasing a frozen wave-form at once as conducted by Nunnally, in dealing with a continuous wave one of ordinary skill in the art may operate or activate Nunnally's photoconductive triggers sequentially under a controlled time-delay as taught by Zucker-203, such that the induced current distribution moves faster than light speed in vacuo, $V_p > c$, as suggested by Bridges, instead of simultaneously, as in Nunnally's ($V_p \rightarrow \infty$). However, as known to one of ordinary skill in the art, the resulting waveform will not propagate along the transmission line at a superluminal velocity, as believed by Applicant, but instead, at a velocity given by the propagation property of the transmission line.

Art Unit: 2881

It would have been further obvious to one of ordinary skill in the art by the time the invention was made to further modify Bridges's device previously modified by Nunnally's, also by Zucker-203's, in order to obtain a quasi-continuous emission of broad-spectrum square-wave trains out of Zucker's horn antenna placed as a load at the end of Nunnally's linear array of capacitors.

Note, although Zucker-203's teaching is not at all necessary to successfully reject claim 23, such a combination is appropriate to establish at least a specific utility while providing a basis for the next dependent claims. This rejection anticipates to have overcome the previously applied § 101 and § 112 rejections based on a lack of general and/or specific utilities.

15. Regarding claims 24 and 28, the limitation that the spectrum of the emitted radiation contains frequencies higher than the modulation frequency of the emitting current is rendered obvious by the fact generally known in the art that a square-wave inherently contains frequencies (much) higher than the base modulation frequency as a result of the many overtones thereby produced.

16. Regarding claim 26, Nunnally's polarizable medium has a rectilinear shape, since it is embedded between the capacitor plates that form a linear sequence.

17. The limitation of claim 27 regarding the accelerated motion of the polarization current distribution is already encompassed in claim 21, whereas the further limitation

Art Unit: 2881

regarding a cusp has been previously rejected as having no significance in the real world, and hence, does not further limit the claim.

18. Insofar the Examiner can ascertain beyond the above rejection under the first and second paragraph of 35 U.S.C. 112, claims 25 and 29 are rejected under 35 U.S.C. 103(a) as being unpatentable over Bridges in view of Fay (USPAT 5,128,687).

Bridges shows all the limitations of claims 25 and 29, as applied previously to the parent claim 21, except the recitation of the polarizable medium having the shape of a circle or an arc of the circle.

Fay discloses an apparatus for generating electromagnetic radiation equipped with polarizable medium in form of radiating elements 24(1) through 24(N) that are arranged in the form of an arc of a circle of radius R, as depicted in Fig.2 and recited in Col.4/ll.44-52. Further, Fay's device is also equipped with phased array 4 consisting of focused phased array antennas 4(1) to 4(T), and still another array 26(1) to 26(T), all arranged on an arc of a circle of radius R, as recited in Col.4/ll.60-68 & Col.5/ll.1-13. Phased array 4 generates a beam 32 that focuses on a point in the near zone, as recited in Col.5/ll.7-13.

Obviously, Fay's device has much more capability than what is claimed by Applicant. However, those unneeded or undesired elements in Fay's device, together with their function(s), may be simply eliminated, since omission of an element and/or its function is obvious if the function of the element is not desired, required or intended. *Ex Parte Wu*, USPQ 2031 (Bd. Pat. App. & Inter. 1989).

Art Unit: 2881

In the alternative, Bridges as modified by Fay discloses the claimed invention except for the use of not less than three phased arrays, each having a different purpose and each being arranged on an arc of a circle, which is also a limitation of Applicant's claim 29. Since applicant has not disclosed that Applicant's single array solves any stated problem or has any particular purpose, it appears that the invention would perform equally well with Fay's three different arrays. Therefore, Applicant's use of a single array is a mere matter of design choice that is unpatentable, because it only involves routine skill in the art. In this respect, it would have been obvious to one of ordinary skill in the art by the time the invention was made to modify Bridges's device by Fay's multiple antenna arrays, in order to have multiple simultaneous beams that can be independently steered, as suggested by Fay in the Abstract.

Communications

19. Any inquiry concerning this communication or earlier communications from the examiner should be directed to Bernard E Souw whose telephone number is ~~703-305-~~ ~~571-272-2482~~ ~~0149~~. The examiner can normally be reached on Monday thru Friday, 9:00 am to 5:00 pm..

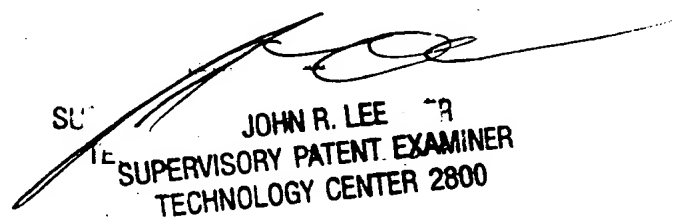
If attempts to reach the examiner by telephone are unsuccessful, the examiner's supervisor, John R Lee can be reached on 703 308 4116. The fax phone numbers for the organization where this application or proceeding is assigned are (703) 872-9306 for regular communications and 703 872 9319 for After Final communications.

Application/Control Number: 09/786,507
Art Unit: 2881

Page 19

Any inquiry of a general nature or relating to the status of this application or proceeding should be directed to the receptionist whose telephone number is 703 308 0956.

bes
October 23, 2003


SU
TE JOHN R. LEE JR
SUPERVISORY PATENT EXAMINER
TECHNOLOGY CENTER 2800